清華大學 Tsinghua University

AIAA Transition Modeling Prediction Workshop-I, 21-22, Jan., 2021; on-line

Transition prediction using the three-equation k-ω-γ transition/turbulence model

Yu PANG, Zhixiang XIAO[α] and Song FU[β]

[α]xiaotigerzhx@tsinghua.edu.cn, AIAA Associate Fellow; [β] AIAA Fellow

School of Aerospace Engineering, Tsinghua University, China

LAMD

Laboratory of Aerodynamics Simulation and preliminary Design for innovative aero-vehicles

LAST

Laboratory for Advanced Simulation of Turbulence

Contents

- Background
- Transition models with intermittency factor
- Overview our previous work
- Results and discussion
- Conclusions

1. Background

- Transition is very important for wind-turbine, high-altitude air-ship, civil airplane and hypersonic aero-vehicle.
  - Larger laminar region always leads to smaller skin friction and heat rates.
- Accurate prediction of transition is a great challenge.
- Prediction methods
  - DNS, DLES ➔ too expensive
  - LST+$e^{N.}$ ➔ difficult to apply in industry
  - Transition model ➔ satisfy the accuracy and cost

CFD Vision 2030

"Perhaps the single, most critical area in CFD simulation capability that will remain a pacing item by 2030 in the analysis and design of aerospace systems is the ability to adequately predict viscous turbulent flows with possible **boundary layer transition** and flow separation present."

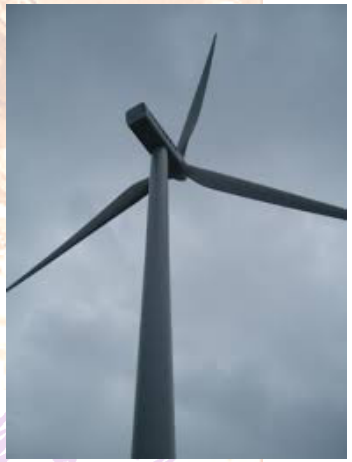

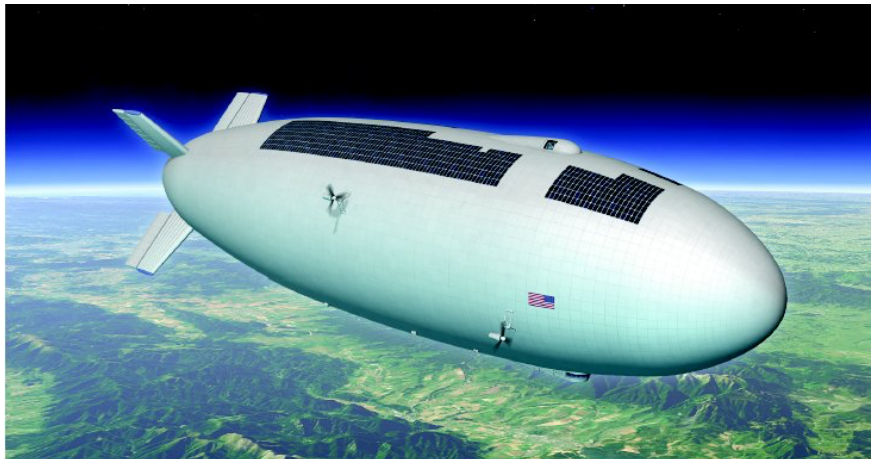

2. Transition models with intermittency factor

- The most popular model is k-**ω**-**γ**-Re_{θ} proposed by Langtry and Menter (2006)

$$\frac{\partial(\rho\gamma)}{\partial t}+\frac{\partial(\rho U_j\gamma)}{\partial x}=P_\gamma-E_\gamma+\frac{\partial}{\partial x_j}\left[\left(\mu+\frac{\mu_t}{\sigma_f}\right)\frac{\partial\gamma}{\partial x_j}\right]$$

$$\frac{\partial(\rho \tilde{Re}_{\theta t})}{\partial t}+\frac{\partial(\rho U_j \tilde{Re}_{\theta t})}{\partial x}=P_{\theta t}+\frac{\partial}{\partial x_j}\left[\sigma_{\theta t}(\mu+\mu_t)\frac{\partial \tilde{Re}_{\theta t}}{\partial x_j}\right]$$

The effective eddy viscosity is combined with the non-turbulent part and the turbulent part by intermittency factor. The non-turbulent eddy viscosity is the product of TKE and the time scale, τ_{nt}, which is the sum of the time scales of the first, second (Mack) and crossflow modes.

- The present model is k-**ω**-**γ** by Fu and Wang (2009, 2013) on basis of LST

$$\frac{\partial(\rho k)}{\partial t}+\frac{\partial(\rho u_j k)}{\partial x_j}=\frac{\partial}{\partial x_j}\left[\left(\mu+\frac{\mu_{eff}}{\sigma_k}\right)\frac{\partial k}{\partial x_j}\right]+P_k-\varepsilon$$

$$\frac{\partial(\rho\omega)}{\partial t}+\frac{\partial(\rho u_j\omega)}{\partial x_j}=\frac{\partial}{\partial x_j}\left[\left(\mu+\frac{\mu_{eff}}{\sigma_\omega}\right)\frac{\partial\omega}{\partial x_j}\right]+P_\omega-D_\omega+Cd_\omega$$

$$\frac{\partial(\rho\gamma)}{\partial t}+\frac{\partial(\rho u_j\gamma)}{\partial x_j}=\frac{\partial}{\partial x_j}\left[\left(\mu+\frac{\mu_{eff}}{\sigma_\gamma}\right)\frac{\partial\gamma}{\partial x_j}\right]+P_\gamma-\gamma P_\gamma$$

$$\mu_{eff}=(1-\gamma)\mu_{nt}+\gamma\mu_t \qquad \mu_{nt}=C_\mu\bar{\rho}k\tau_{nt} \qquad \tau_{nt}=\tau_{nt,2d}+\tau_{cross}$$

$$\tau_{nt,2d}=\begin{cases}\tau_{nt1}, |M_{rel}|\le 1\\ \tau_{nt1}+\tau_{nt2}, |M_{rel}|>1\end{cases}$$

$M_{rel}=(U-c_r)/a$, 当地相对马赫数

$$\tau_{nt1}=C_2\zeta_{eff}^{1.5}\Big/\left[(2E_u)^{0.5}\nu\right]^{0.5} \qquad \zeta_{eff}=\min(\zeta,C_1 l_T)$$

$$\tau_{nt2}=C_3\times 2\,\zeta_{eff}\Big/U(y_s) \qquad \tau_{nt2,new}=C_{3,new}\left(\frac{\mathrm{Re}_{local}}{\mathrm{Re}_\infty}\right)^{C_0}\tau_{nt2}$$

$$\tau_{cross}=C_7 g\left(4\zeta_{eff}/U_e\right)\times\left\{1-\exp\left[-C_8\left(\zeta_{eff}U_e/\nu_e-44\right)^2\right]\right\}\times\left(W/U_e\right)^{C_9}$$

$$P_\gamma=C_4\rho f(\mathrm{Tu})F_{onset}\left[-\ln(1-\gamma)\right]^{0.5}\left(1+C_5\frac{k^{0.5}}{(2E_u)^{0.5}}\right)\frac{d}{\nu}|\nabla E_u|$$

$$F_{onset}=1.0-\exp\left(-C_6\frac{\zeta_{eff}k^{0.5}|\nabla k|}{\nu|\nabla E_u|}\right) \qquad f(Tu)=\sqrt{1.25\times10^{-11}Tu^{7/4}}$$

3. Overview our previous work

Ma	*Re*(/m)	*T*(K)	α (°)	*FSTI* （%）
0.147	3.3E6	293	0	0.18

Ma	*Re*(/m)	*T*(K)	T_w(K)	α (°)	*FSTI* （%）
6.2	2.6E6	690.0	290	0	0.32

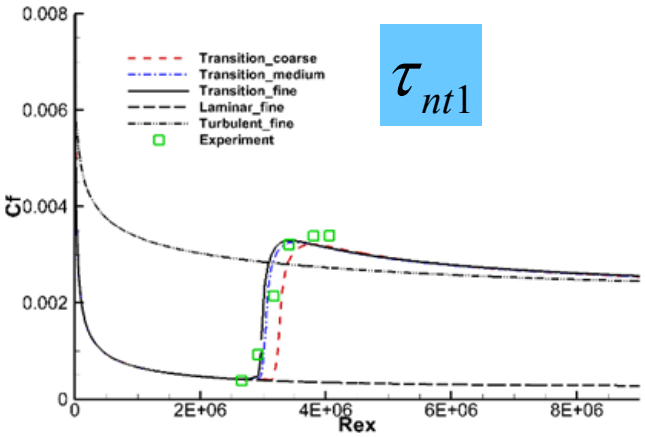

τ_{nt1}

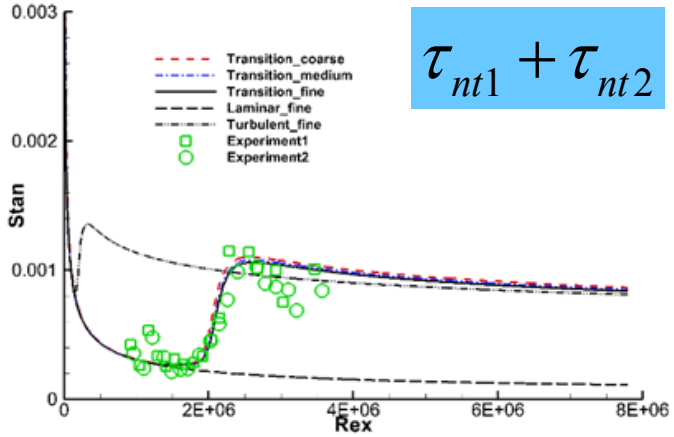

$\tau_{nt1} + \tau_{nt2}$

This model was validated by some typical cases, such as the transition past the low-speed flat plate, dominated by 1st mode; the hypersonic flat plate dominated by the 1st and 2nd modes; the swept wing dominated by the 1st and crossflow modes.

NLF(2) 0415, Re=3.73E6, AOA= -4,FSTI=0.05%

Yang, Wang, Xiao & Fu, EUCUSS, 2017

$\tau_{nt1} + \tau_{cross}$

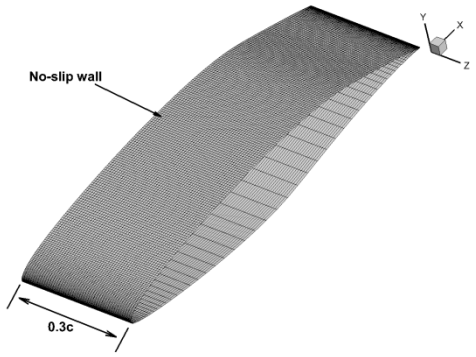

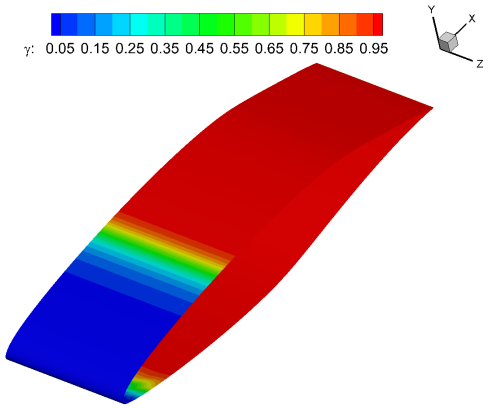

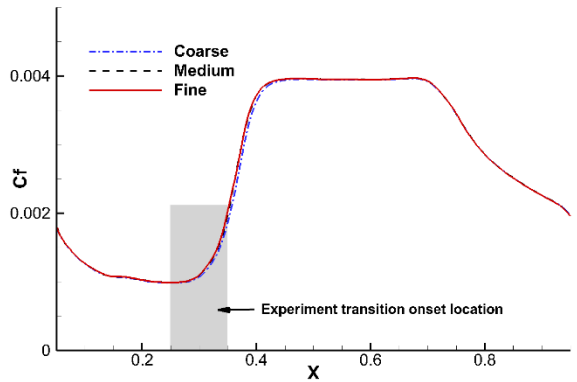

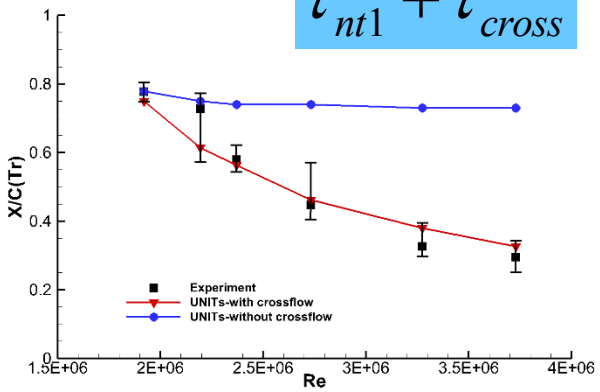

$$\tau_{nt2,new} = C_{3,new}\left(\frac{\mathrm{Re}_{local}}{\mathrm{Re}_{\infty}}\right)^{C_0}\tau_{nt2}$$

R_n/mm	Ma_∞	$Re_{\infty N}$ (/m)	T_∞(K)	α (°)	*FSTI* （%）	Grid
9.53	9.79	1.63E5	51.0	1, 2	0.238	325×89×89

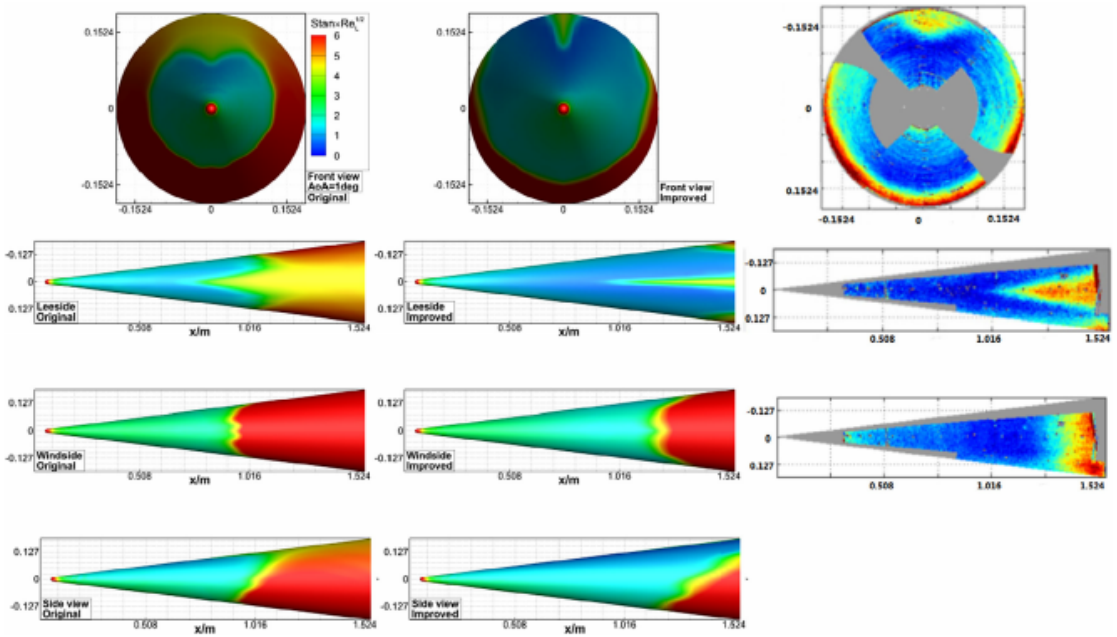

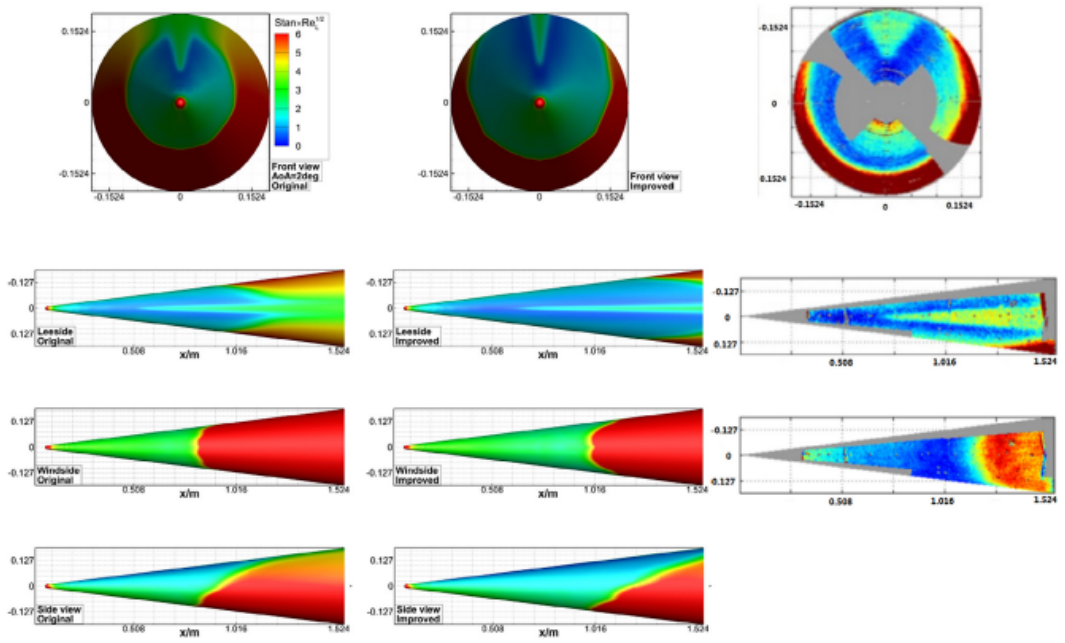

Fig. 14. Comparisons of Stan × $Re_L^{1/2}$ on the wall at AoA = 2 deg.

$\tau_{nt1} + \tau_{nt2,new} + \tau_{cross}$

$Stan \times Re_L^{1/2}$ （Left: α = 1°， Right: α = 2°）

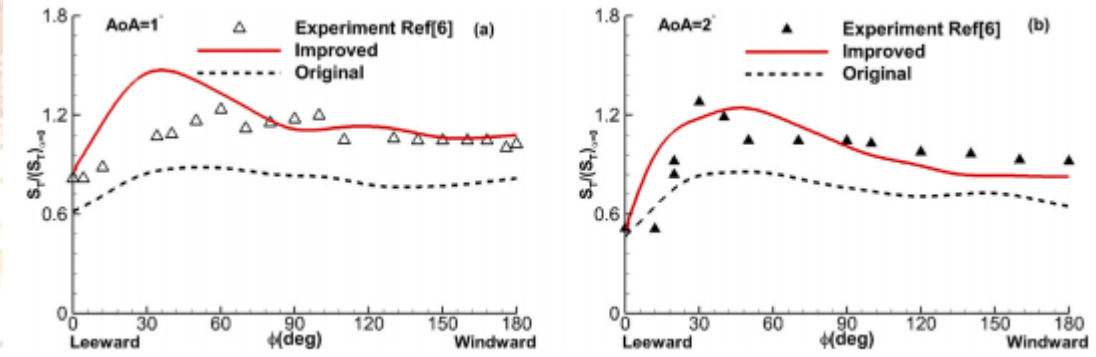

Fig. 15. Relative transition onsets location in the circumferential direction for the two AoAs.

We also simulated the transition past the hypersonic cone with small AoAs.
In this case, the transition is dominated by the first, second and crossflow modes.

Wang G , Yang M , Xiao Z , IJHMT, 2018

Unsteady transition

- The unsteady transition past the oscillating NACA0012
  - U_∞=50m/s, Re_C=1.0E6, α_0=4.46°, $\alpha=\alpha_0+\alpha_m\sin(2k_pt)$, α_m=1.34°, $kp = \omega_p C/2U_\infty$
    - kp=0.075, kp=0.151
- The simulations match the e^N well, with some difference from the Exp.

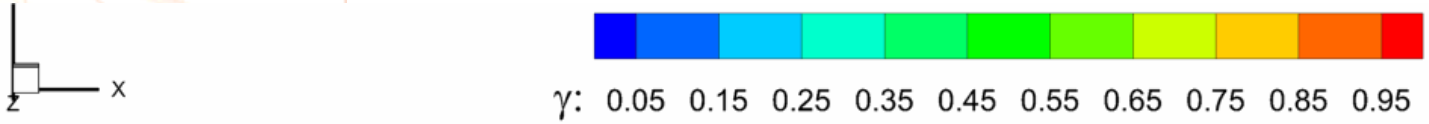

Liu J , Xiao Z , Fu S . AIAA Journal, 2018

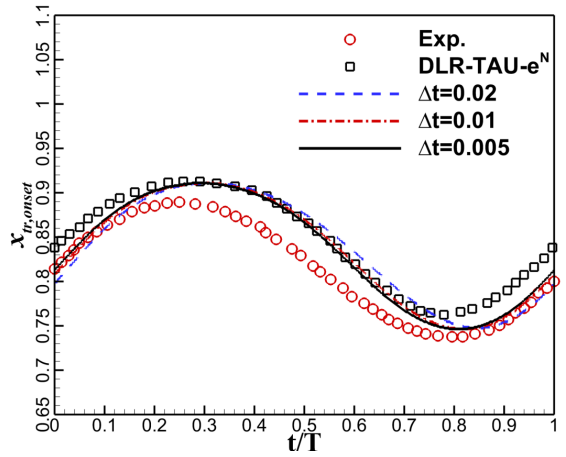

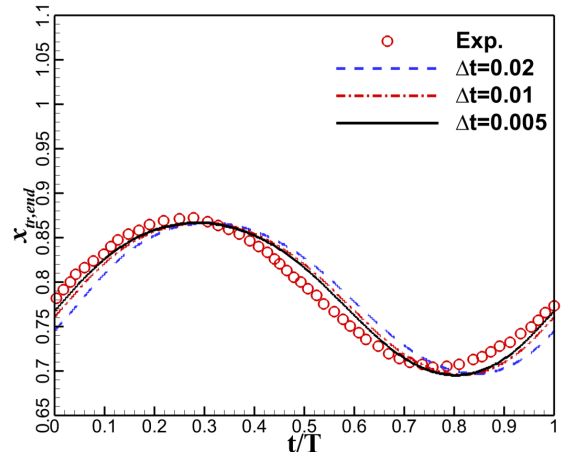

4-equ. transition model

Yang MC, Xiao ZX. Renewable Energy, 2019

- Introducing the roughness amplify factor Ar

$$\frac{\partial(\rho A_r)}{\partial t}+\frac{\partial(\rho u_j A_r)}{\partial x_j}=\frac{\partial}{\partial x_j}\left[\left(\mu+\sigma_{ar}\mu_{eff}\right)\frac{\partial A_r}{\partial x_j}\right]$$

$$A_r\big|_{wall}=\frac{100}{1+e^{-0.7k^+ +10}}$$

$$\xi_{eff,new}=f(A_r)\xi_{eff,old}$$

$$\xi_{eff,old}=\min\left(\frac{d^2\Omega}{U},C_1 l_T\right)$$

$$f(A_r)=1+0.25\times A_r^{0.7}$$

$$\tau_{nt1}=g(Tu)\zeta_{eff}^{1.5}\Big/\left[(2E_u)^{0.5}\nu\right]^{0.5}$$

We also proposed a 4-equ transition model accounting for the effects of distributed roughness.

The transitions past the rough flat plate and DU96 were simulated to validate the new model.

Flat plate with small roughness on the whole surface

Re_∞(m)	Ma	k_s(μm)	Tu (%)
6.65E6	0.2	0,10, 20, 30, 40, 50	1.0

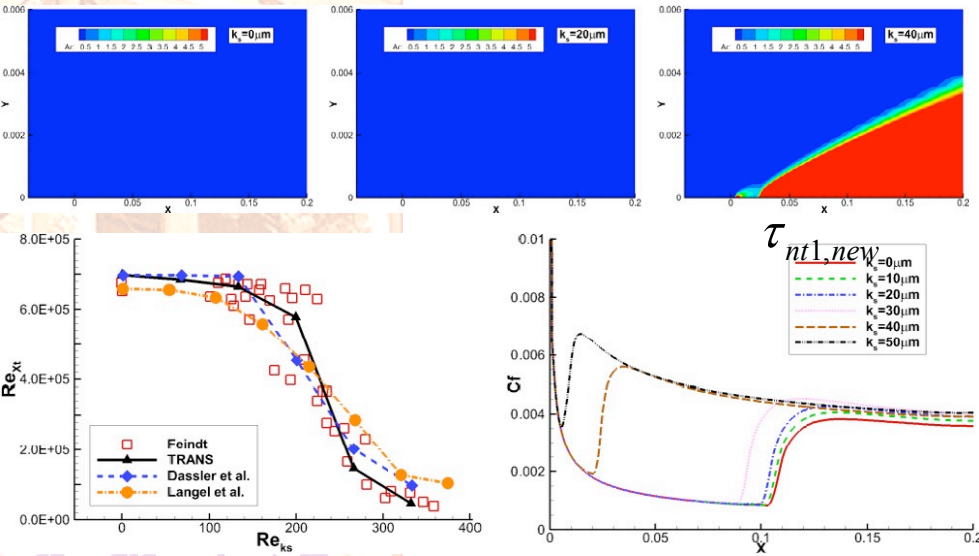

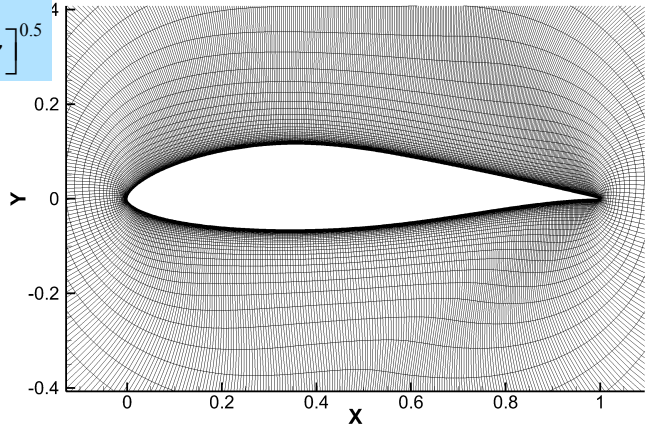

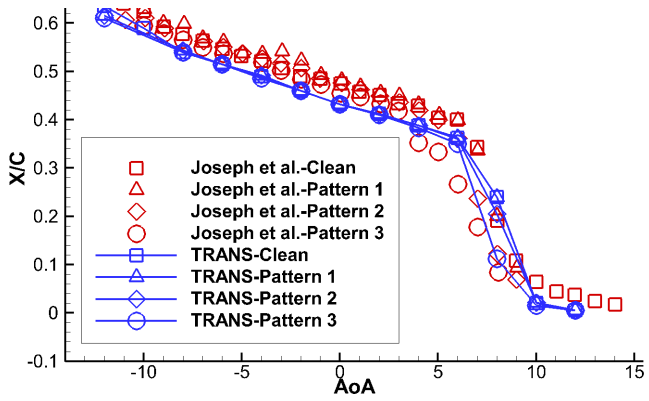

Rough DU96-W-180

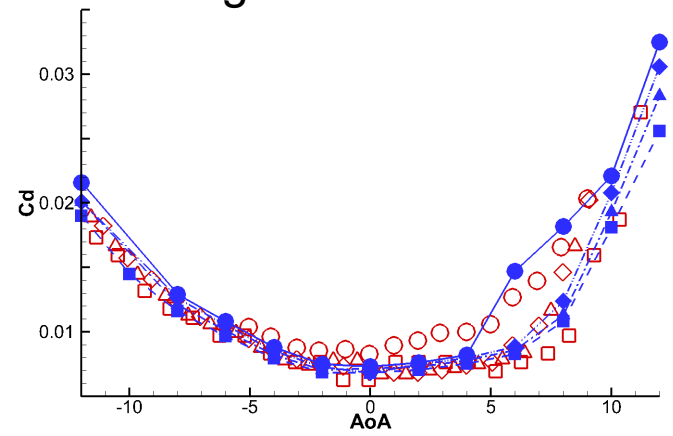

RANS-LES-Tr for transition and separation

Laboratory of Aerodynamics Simulation and preliminary Design for innovative aero-vehicles

Cui & Xiao, Energy, 2020

1st

IDDES-Tr

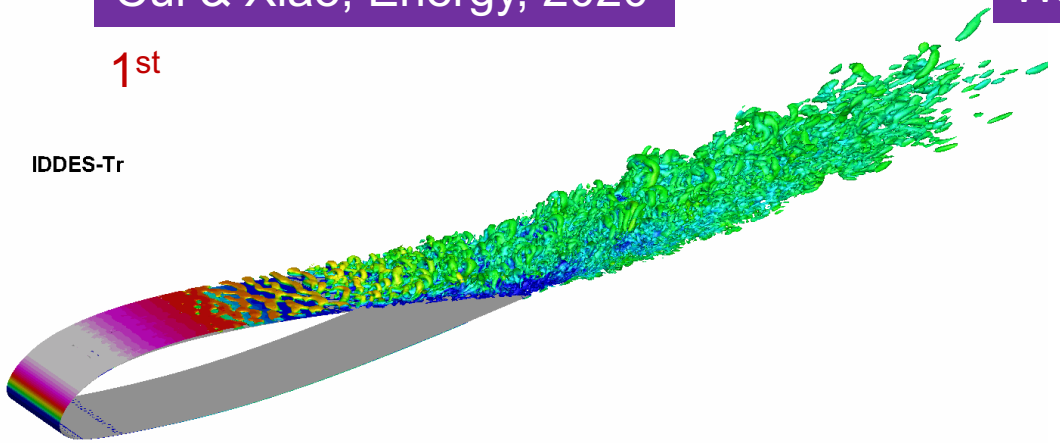

Wang & Xiao, AST, 2020

IDDES-Tr

1st+Crossflow

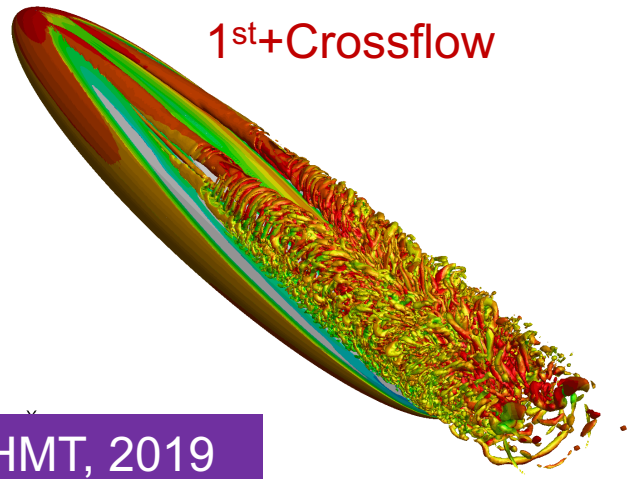

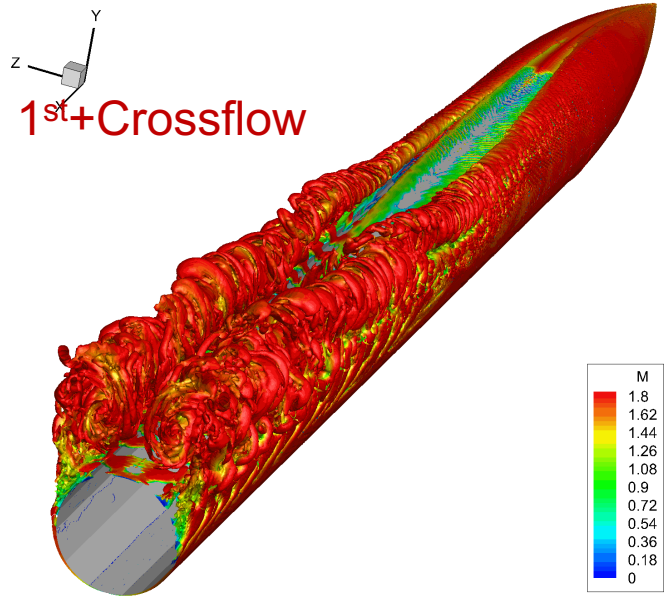

Xiao & Wang, IJHMT, 2019

1st+2nd+Crossflow

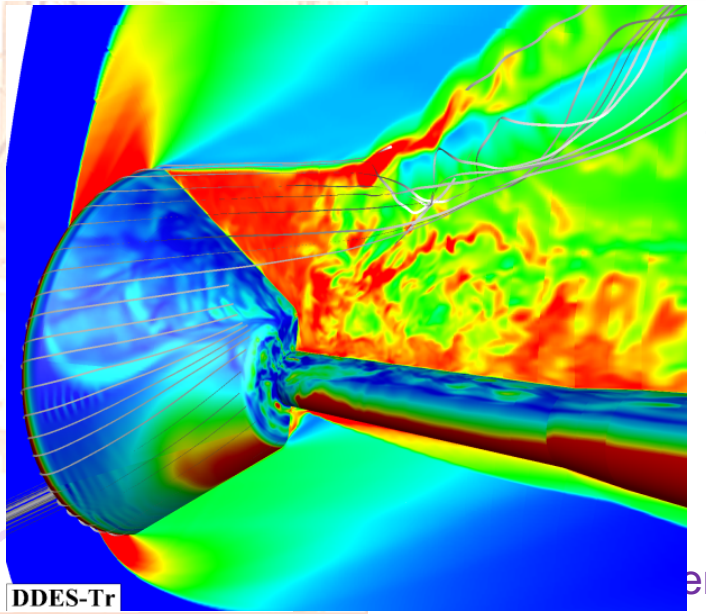

RANS-LES hybrid models based on the transition model were proposed and validated.
It was applied to simulate the transition on the windward side and resolve the separation on the leeward side simultaneously, such as A-Afoil, prolate spheroid, slender body and capsule.

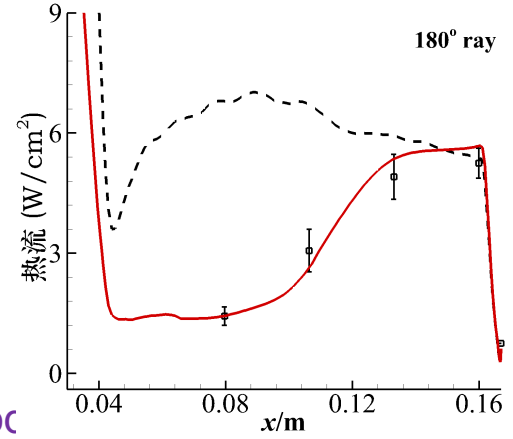

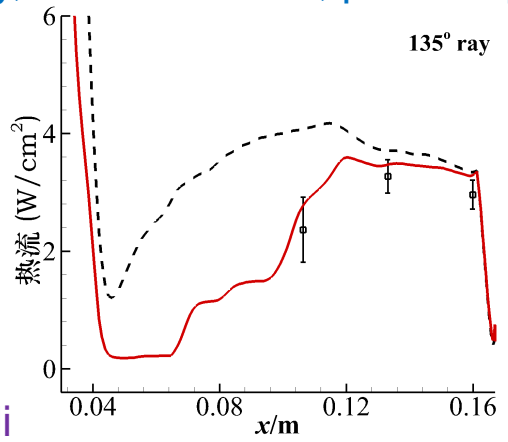

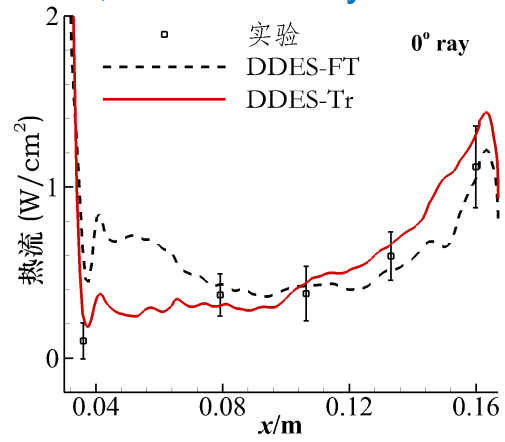

Some publications based on this model

1. ***Fu S***, Wang L. Modelling flow transition in a hypersonic boundary layer with Reynolds-averaged Navier-Stokes approach. Science in China (Series G: Physics, Mechanics & Astronomy), 2009, 05: 768-774.
2. Wang L, ***Fu S***, Carnarius A, et al. A modular RANS approach for modelling laminar–turbulent transition in turbomachinery flows. International Journal of Heat and Fluid Flow, 2012, 34(4): 62-69.
3. ***Fu S***, Wang L. RANS modeling of high-speed aerodynamic flow transition with consideration of stability theory. Progress in Aerospace Sciences, 2013, 58(2): 36-59.
4. Wang L, Xiao LH, ***Fu S***. A modular RANS approach for modeling hypersonic flow transition on a scramjet-forebody configuration. Aerospace Science and Technology, 2016, 56: 112-124.
5. Zhao M, ***Xiao ZX*** and **Fu S**, Predictions of transition on a hovering tilt-rotor blade, *AIAA Journal of Aircraft*, 51(6), 1094-1103, 2014.
6. Liu J, ***Xiao Z*** , **Fu S** . Unsteady Transition Studies over a Pitching Airfoil Using a k-ω-γ Transition Model[J]. AIAA Journal, 2018:1-6.
7. Wang GX, Yang MC, ***Xiao ZX***, **Fu S**. Improved k-ω-γ transition model by introducing the local effects of nose bluntness for hypersonic heat transfer. International Journal of Heat and Mass Transfer, 2018, 119: 185-198.
8. Yang MC and ***Xiao ZX***. Distributed roughness induced transition on wind-turbine airfoils simulated by four-equation k-ω-γ-Ar transition model. Renewable Energy, 2019, 135: 1166-1177
9. Yang MC & ***Xiao ZX***. POD-based surrogate modeling of transitional flows using an adaptive sampling in Gaussian process. *Int Journal of Heat and Fluid Flow*. 84, 108596, 2020
10. Yang MC, **Xiao ZX**. Parameter uncertainty quantification for a four-equation transition model using a data assimilation approach. Renewable Energy, 2020.
11. Yang MC, **Xiao ZX**. Improving the k-ω-γ-Ar transition model by the field inversion and machine learning framework. Physics of Fluids, 2020.
12. ***Xiao ZX,*** Wang GX, Yang MC, Chen LZ. Numerical investigations of hypersonic transition and massive separation past Orion capsule by DDES-Tr. International Journal of Heat and Mass Transfer, 2019, 137: 90-107
13. Wang GX, ***Xiao ZX*** & Chen LZ. Simultaneous simulation of transition and massive separation by RANS-LES-Tr model. *Aerospace Science and Technology*, 105, 106026, 2020.
14. Cui WY, ***Xiao ZX*** & Yuan XJ. Simulations of transition and separation past a wind-turbine airfoil near stall. *Energy*, 205, 118003, 2020.

TRANsition and Turbulence ***S***olver (TRANS)

In-house compressible FVS Navier-Stokes solver

- Grid: **Multi-block structured grid**
- Patch：**P-to-P**, quasi-p-to-p and overset
- Spatial schemes：Jameson type central with artificial viscosity、Roe、van Leer、STVD、AUSMPW+、 **AUSM+-up**
  - MUSCL or WENO interpolation,
  - MDCD-WENO
  - Adaptive dissipation
- Time marching：Runge-Kutta, **LU-SGS-τTS**
- Transition/turbulence models：**k-ω-γ transition/turbulence model**, S-A, k-g/**k-ω-SST**/Wilcox-1988/1998/2006, CC, RG-EARSM
- RANS/LES：DDES/IDDES based on k-ω-γ modelDNS
- Parallel:**MPI**
- Has been validated by many standard models.

4. Results and discussion

- Fully Turbulent 3D Bump-in-Channel (FT)
- Zero-Pressure-Gradient Flat Plate (1st)
- NLF(1)-0416 Airfoil (1st)
- 6:1 Prolate Spheroid (1st + crossflow)
- CRM-NLF wing-body (Preliminary results) (1st + crossflow)

CASE0. FT 3D Bump-in-Channel

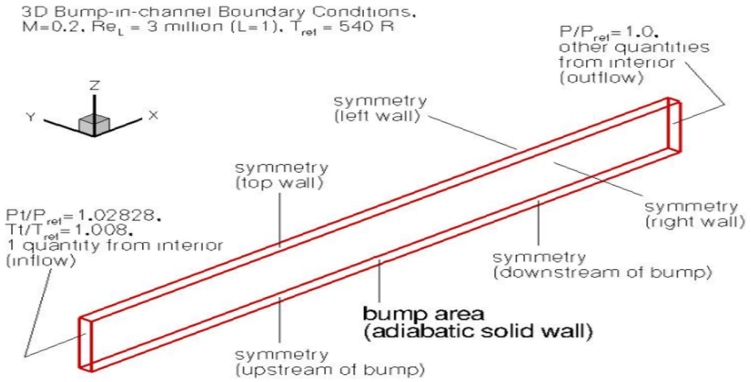

- Computational & Boundary Conditions
  - Ma=0.2, AOA=0, T_∞=300K, Re_L=3.0E6
  - Grids: Spanwise-Streamwaise-Normal
    - LV1: 65x705x321
    - LV2: 33x353x161
    - LV3: 17x177x81
    - LV4: 9x89x41
    - LV5: 5x45x21
- Grid convergence is achieved by LV2
- TRANS performs similar with CFL3D

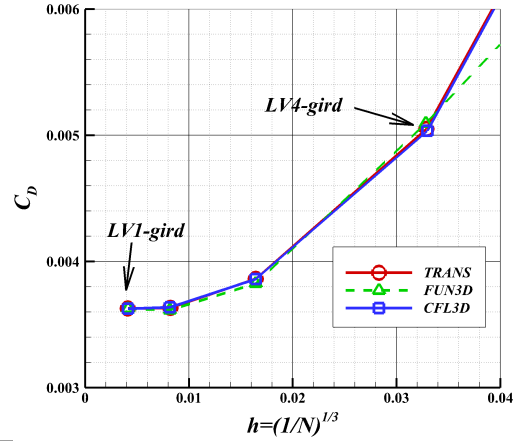

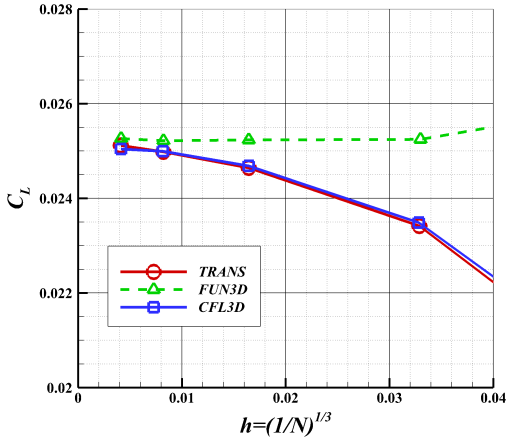

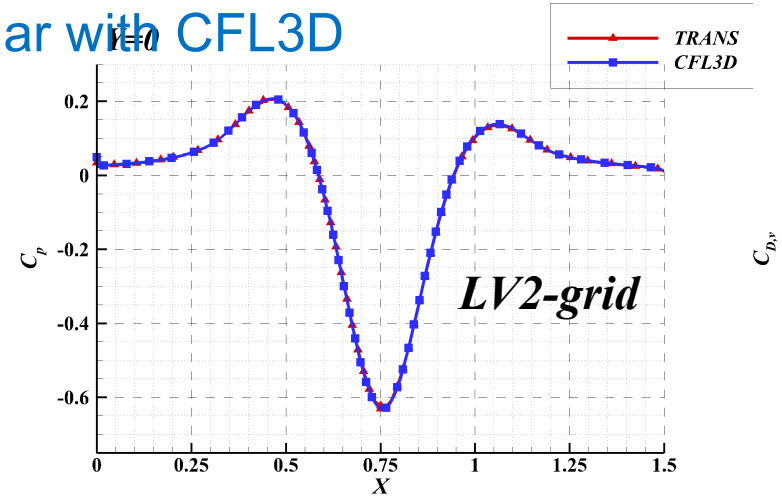

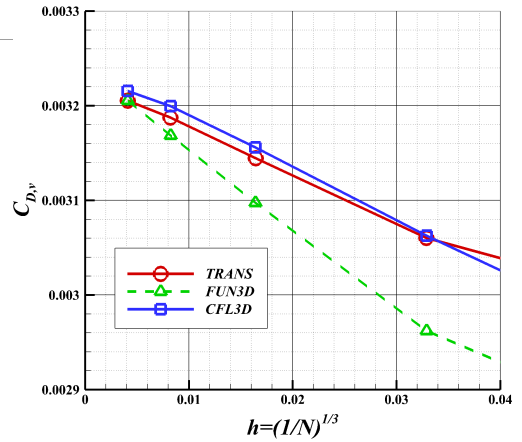

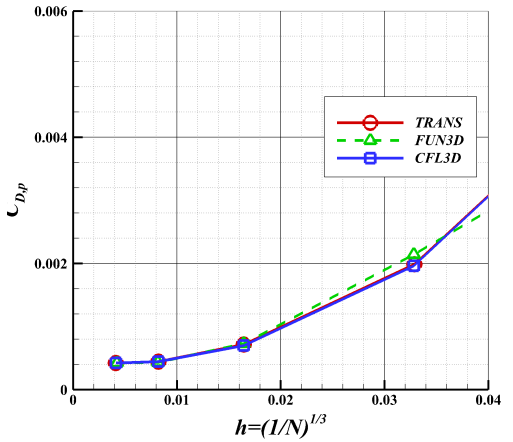

C_p, u_{ref}, v_{ref}, w_{ref}, μ_t/μ_{ref}

- x=1.208 ; y=-0.125
  - LV2-grid: 33×353×161; TRANS, CFL3D
- TRANS performs almost the same with CFL3D, except the eddy viscosity, with different SST and SA turbulence model.

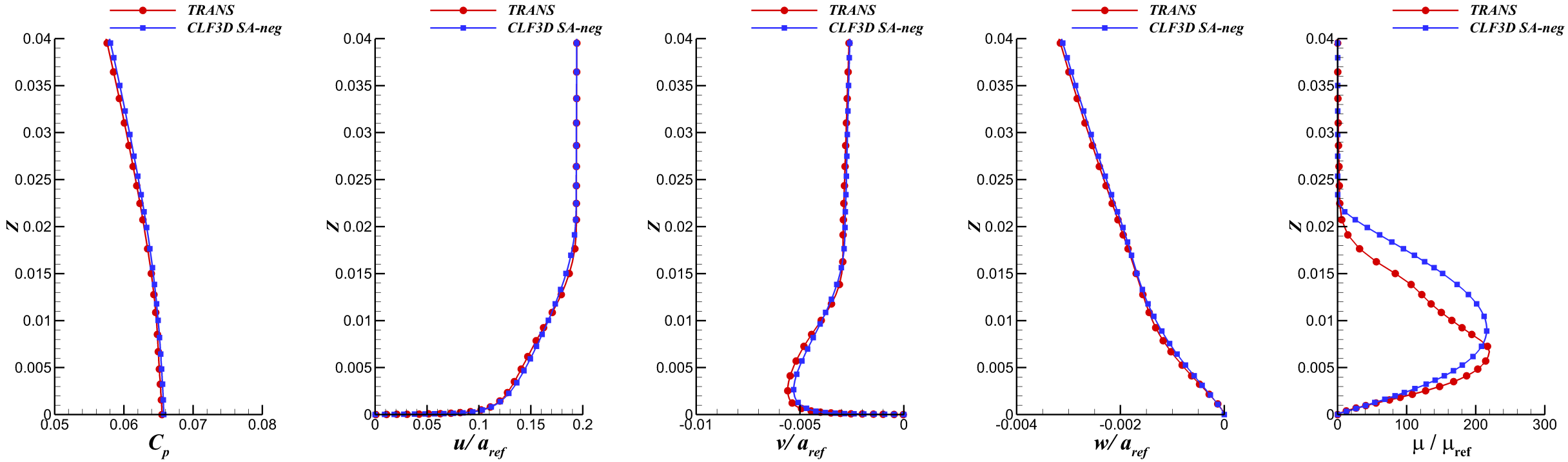

k/a_{ref}^2

- X=0.3 & 1.2, LV2-grid: 33×353×161 ; TRANS, CFL3D, FUN3D

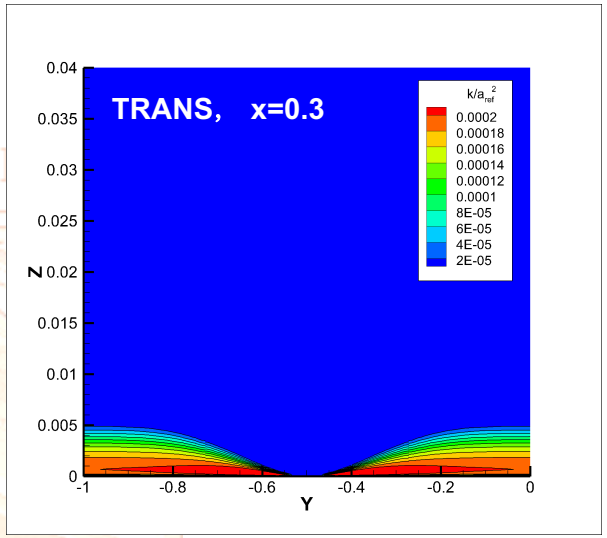

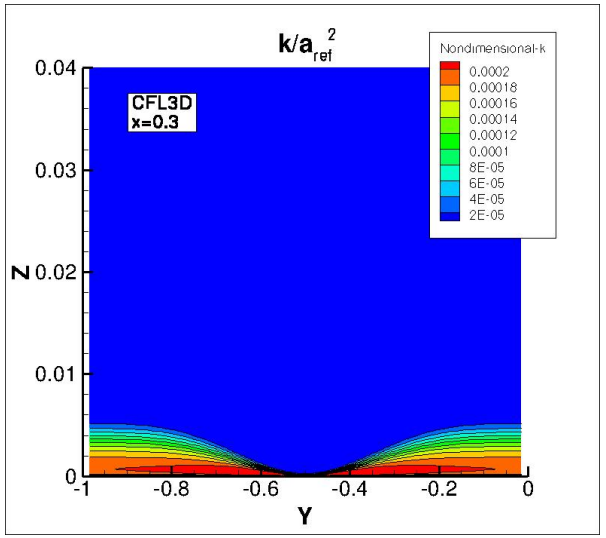

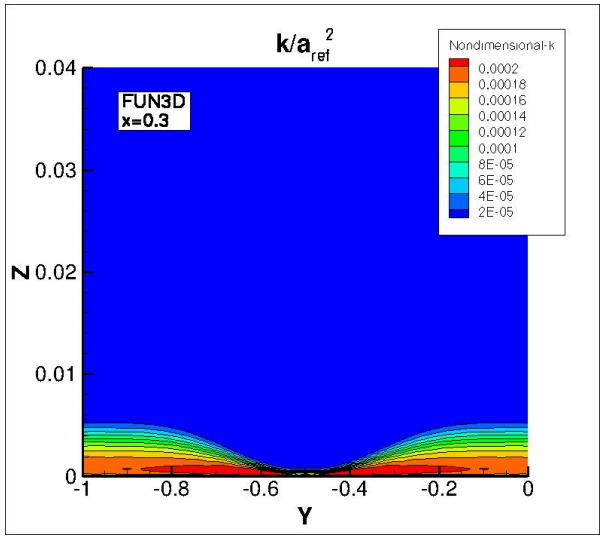

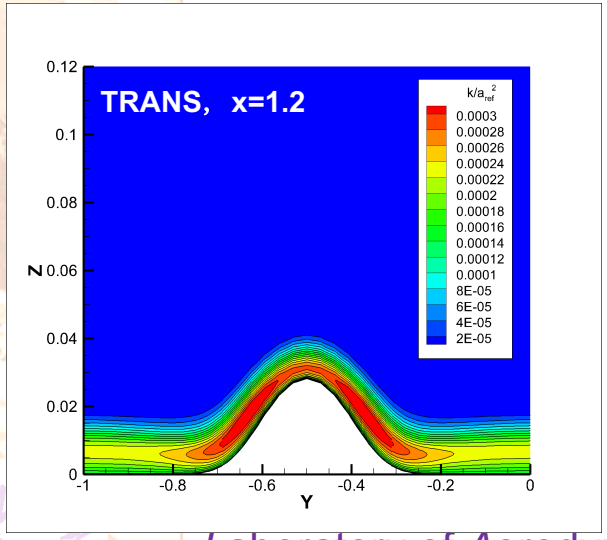

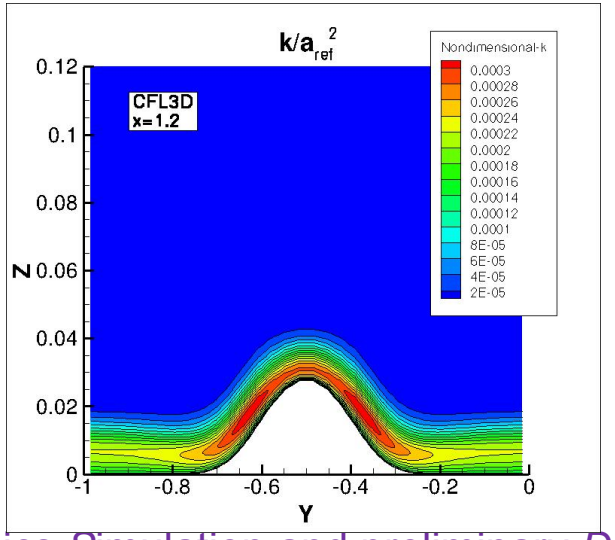

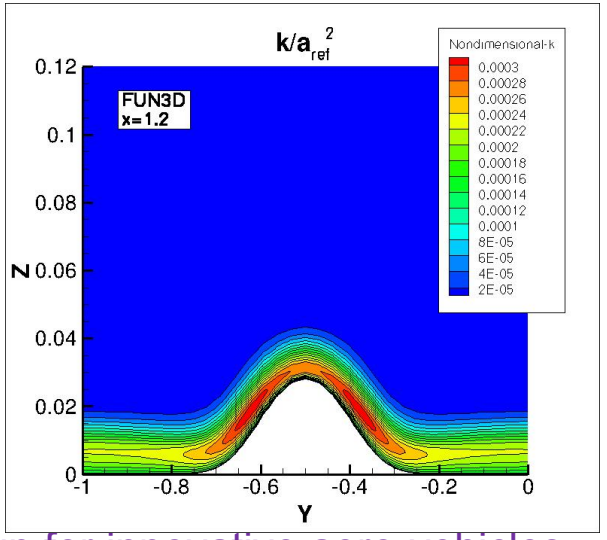

μ_t/μ_{ref}

- X=0.3 & 1.2 ； LV2-grid: 33×353×161 ; TRANS, CFL3D, FUN3D

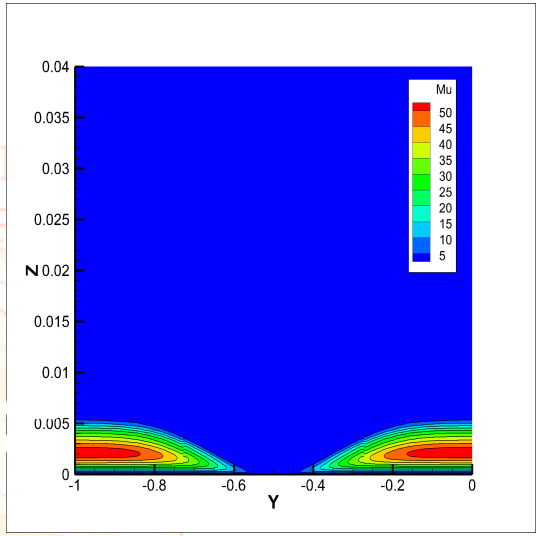

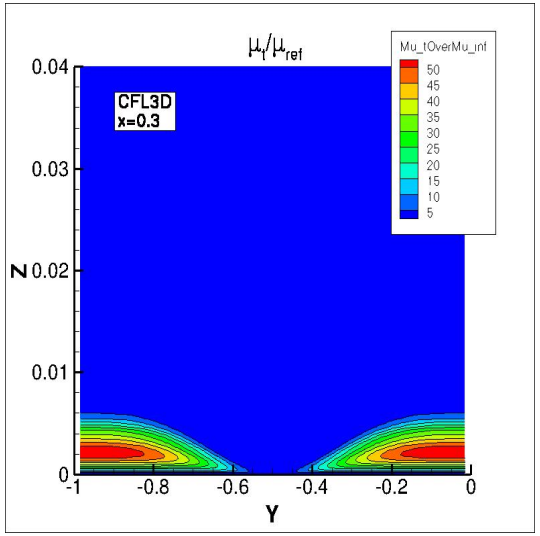

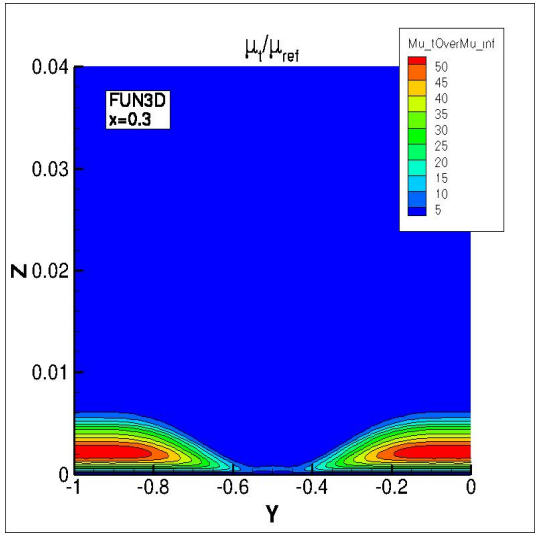

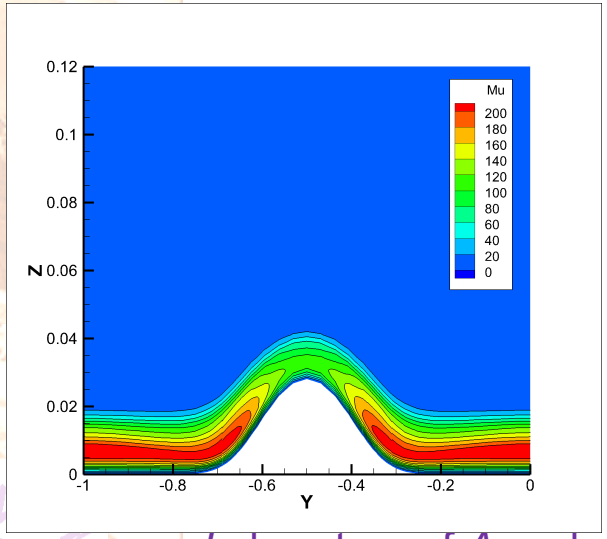

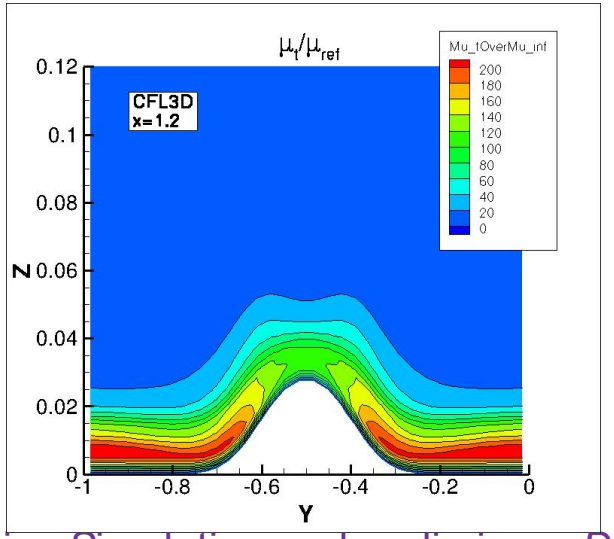

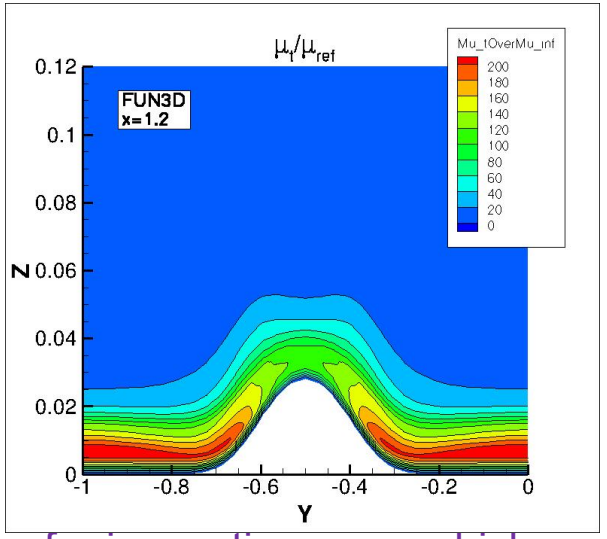

CASE1. Zero-Pressure-Gradient Flat Plate

- Ma=0.2, AOA=0, T_∞=300K, Re_∞=2.0E6 /m,
  - T3A FSTI=5.855%, μ_T/μ = 11.9
  - T3B FSTI=7.216%, μ_T/μ = 99

These two flows are typical by-pass transition with large FSTI and mainly dominated by 1st mode

- Grid Family & Boundary Conditions

Name	N	Streamwise	Normalwise
(**T**)iny	1,125	45	25
(**C**)oarse	4,361	89	49
(**M**)edium	17,169	177	97
(**F**)ine	67,584	353	193
e(**X**)tra fine	270,336	705	384

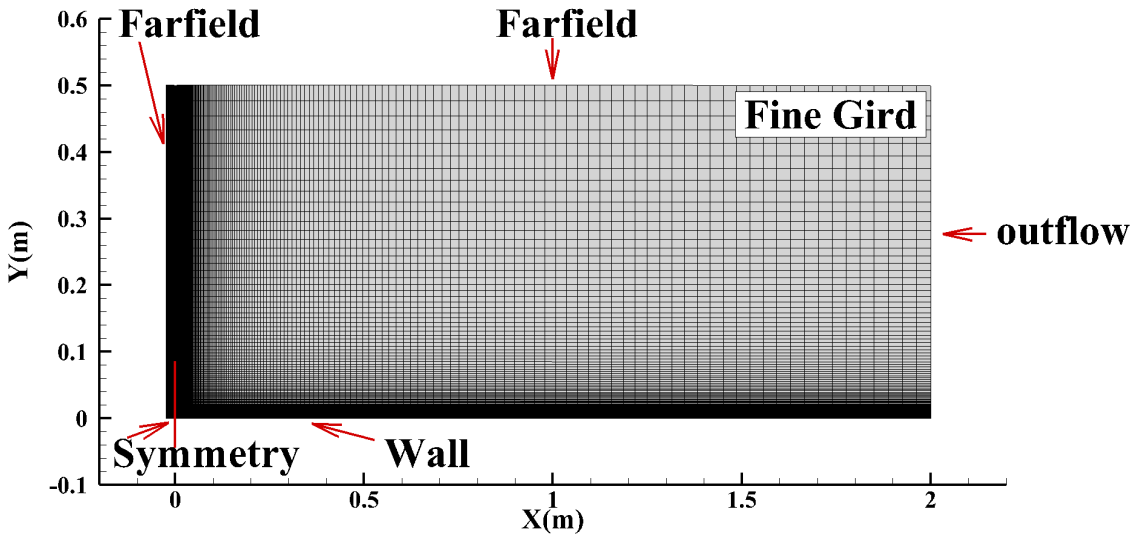

Grid convergence T3A&B

- T3A&B FSTI=5.855% & 7.216%

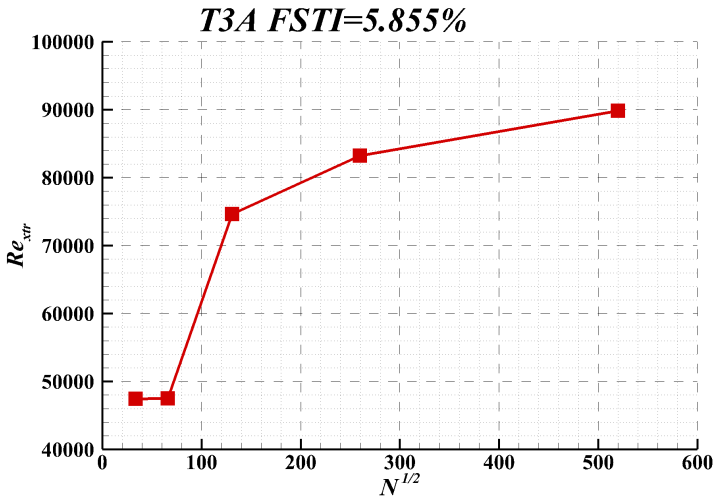

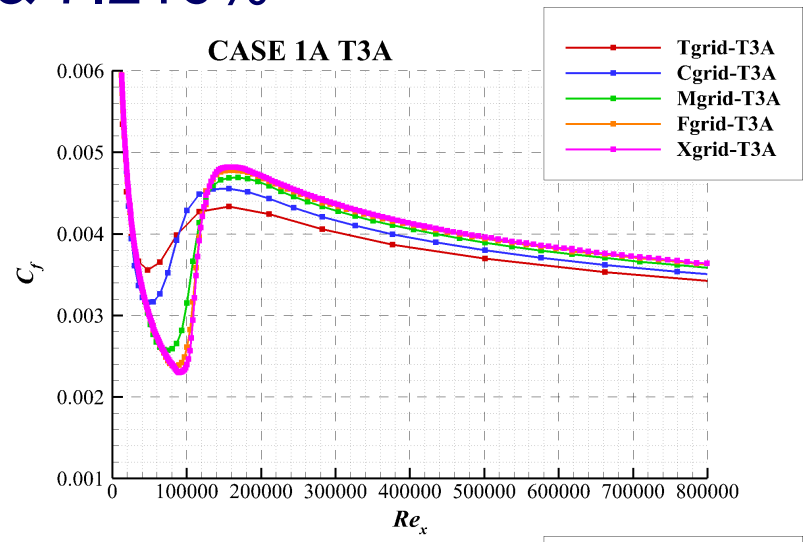

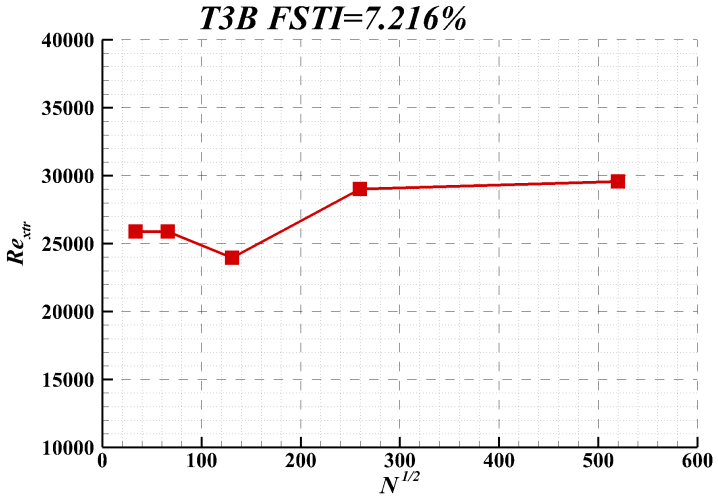

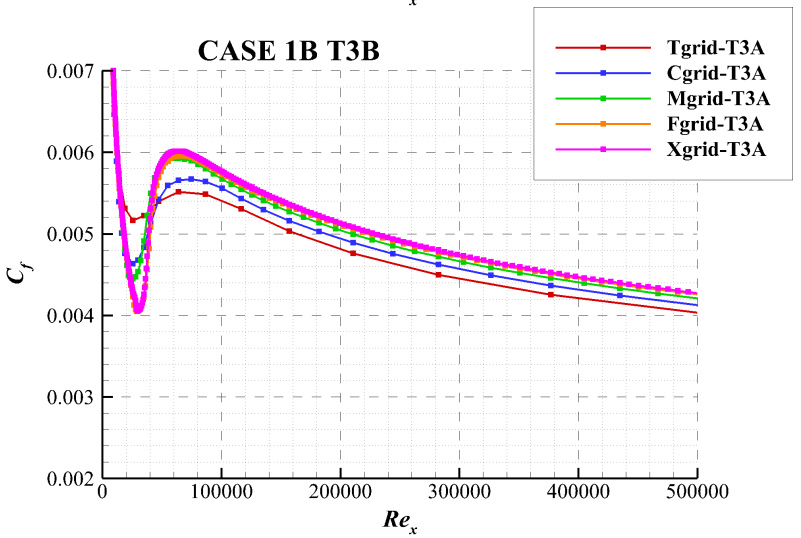

- Fine mesh performs similar with extra-fine mesh, but it's not enough. It means that the grid convergence is not fully achieved.
- Then, the XFine-mesh is applied.
- The transition onset moves downstream and transition range becomes narrower with increase of grid number.

Transition with 4 FSTI

Menter F R , Langtry R B , Likki S R , et al. A Correlation-Based Transition Model Using Local Variables—Part I: Model Formulation[J]. Journal of Turbomachinery, 2006, 128(3):413.

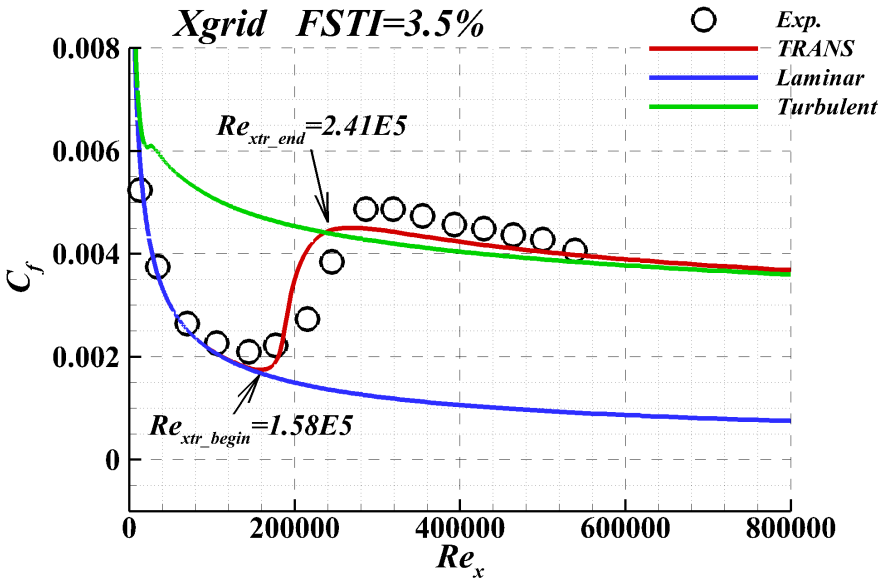

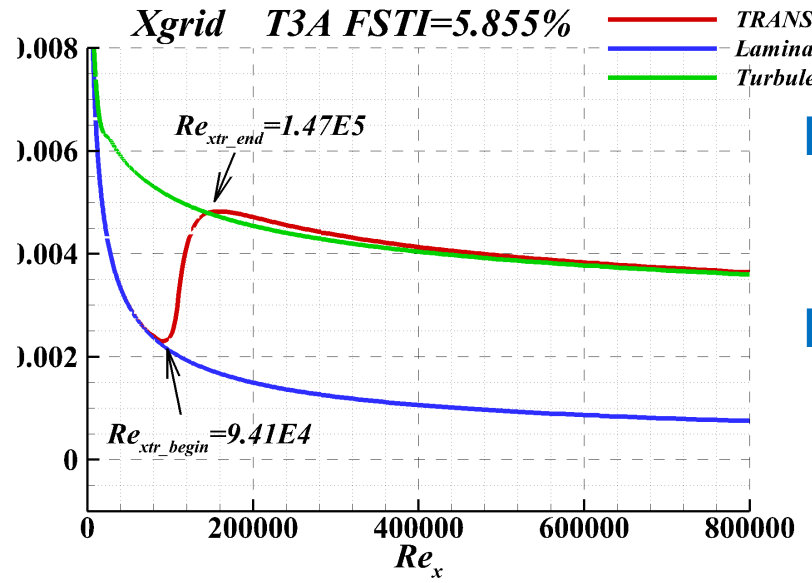

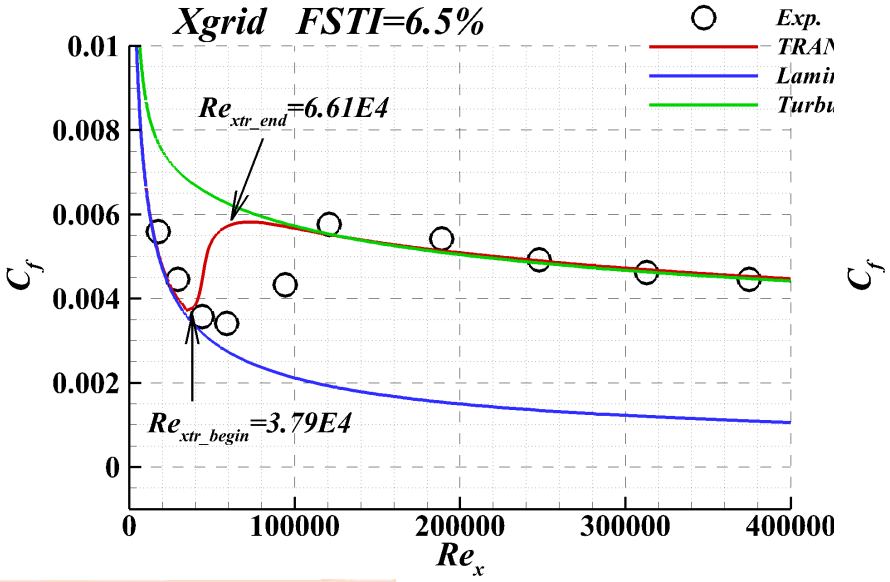

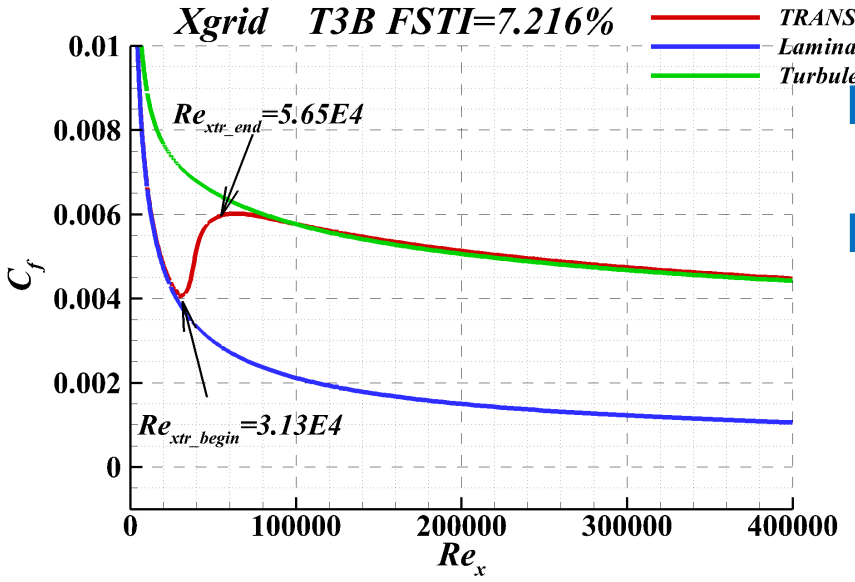

- Two extraordinary cases with Exp. Data are modelled and compared;
- With increase of FSTI, the transition onset moves upstream. Transition onset Re_X varies from 158E3 to 94.1E3 to 37.9E3 to 31.3E3
- The numerical transition range is narrower than exp.
- The difference between simulations and exp. becomes larger with increase of FSTI.

Comparisons of k & γ

- FSTI 5.855% VS 3.5%

The γ can be applied to indicate the transition onset. At the same time, the TKE grows rapidly after the transition.

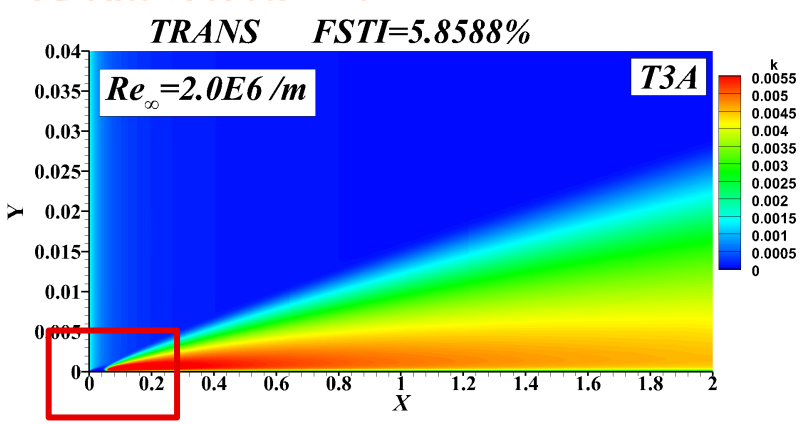

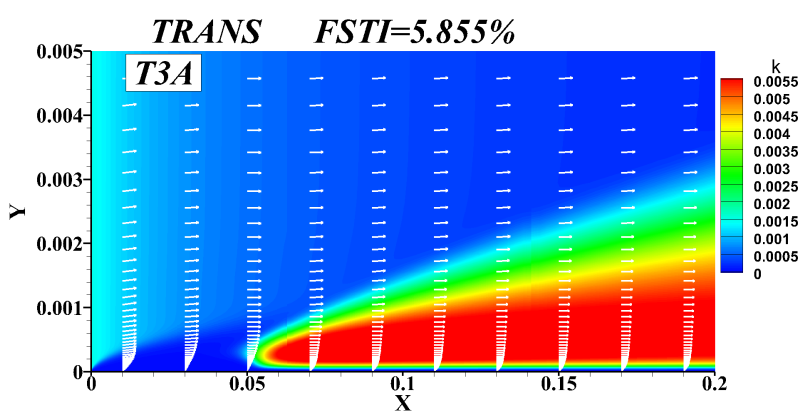

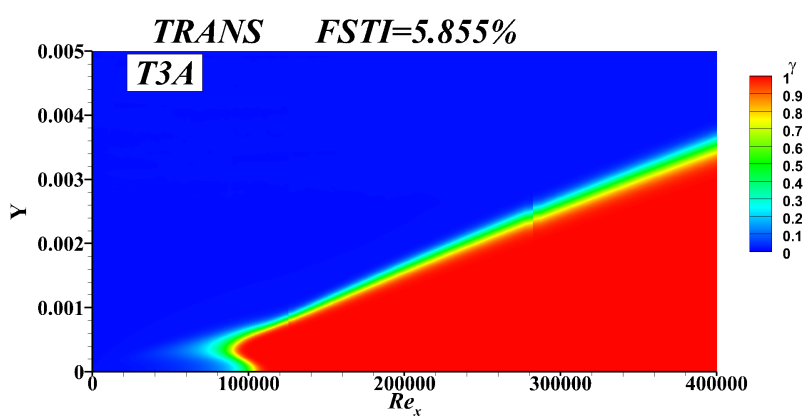

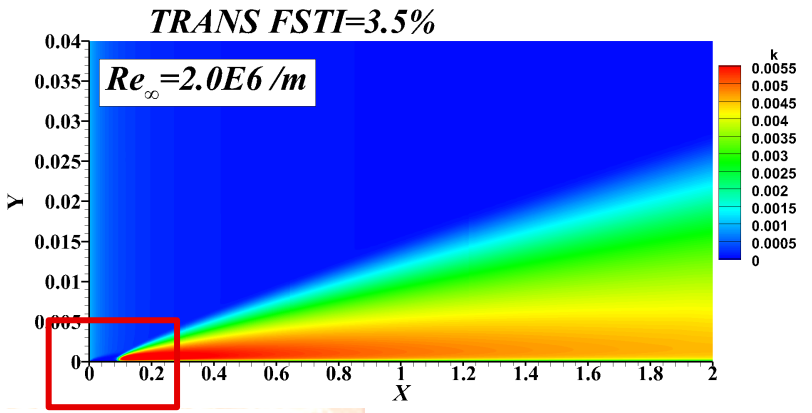

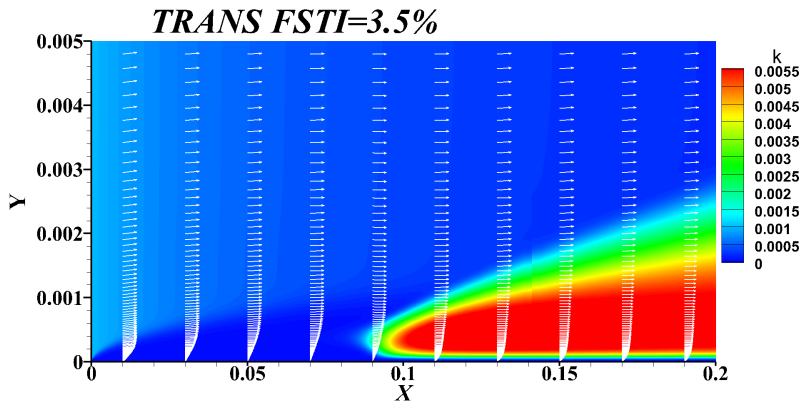

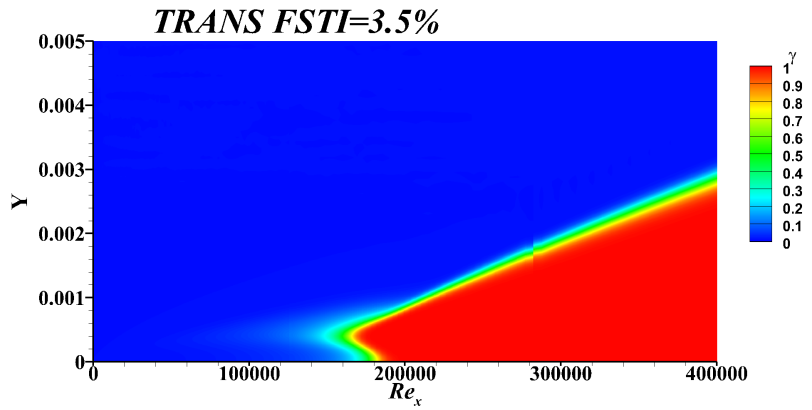

CASE2. NLF(1)-0416 Airfoil

- Computational conditions
  - Ma=0.1, FSTI=0.15%, T_∞=300K, Re_C=4.0E6
    - CASE2A AOA=0, 5 deg.
    - CASE2B AOA=-4, -2, 0, 2, 4, 6, 8 deg.

The flow is the typical natural transition and dominated by 1st mode

- Grid family & Boundary Conditions
  - Wall & Farfield
    - Farfield > 100C

Name	N	Streamwise on surface	Normalwise
(**C**)oarse	40,354	385	88
(**M**)edium	87,040	513	137
(**F**)ine	153,670	769	162

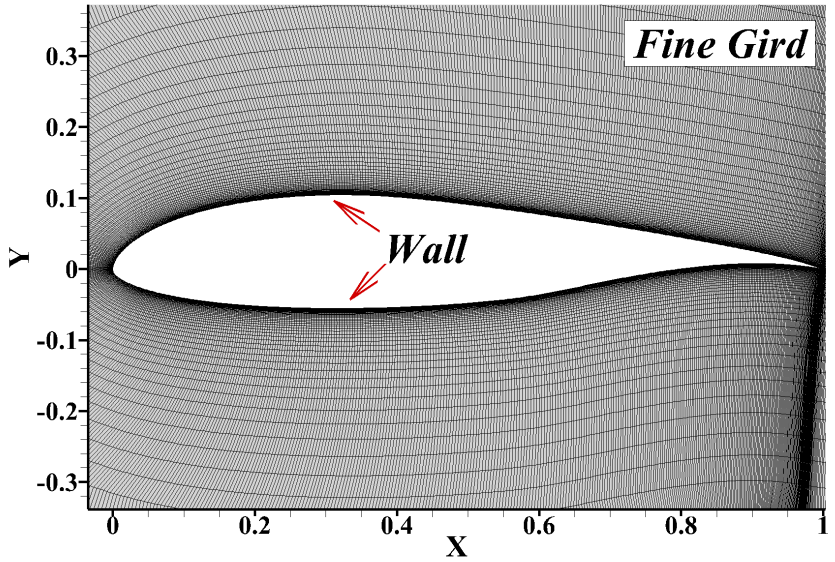

AoA=0deg

Exp. Data: D.M. Somers, Design and Experimental Results for a Natural Laminar Flow Airfoil for General Aviation Applications, 1981. NASA TP 1861.

- The grid convergence is achieved
  - The max. difference of transition onset between the simulation and Exp. is less than 5%C

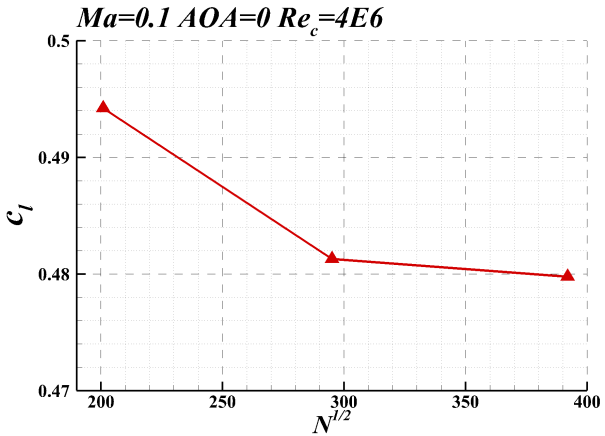

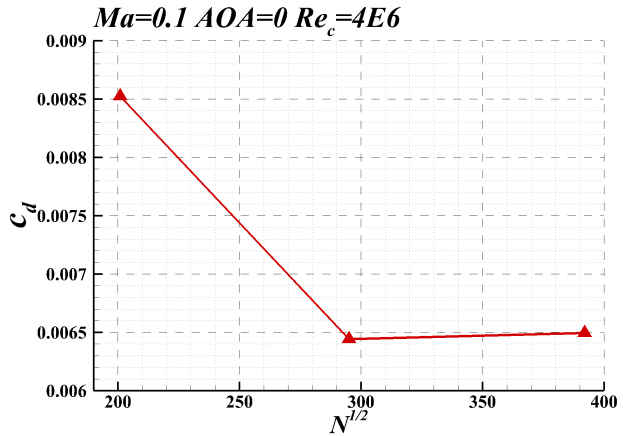

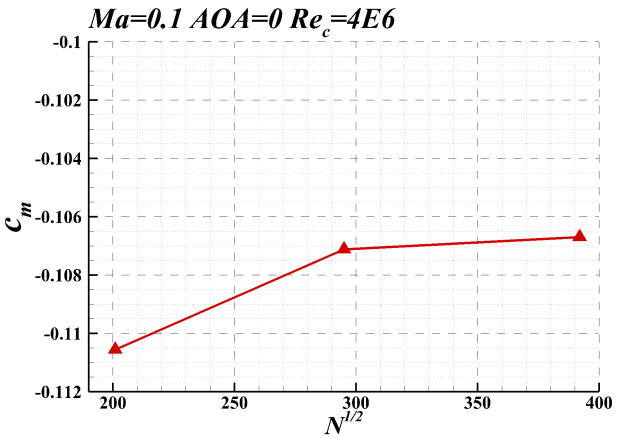

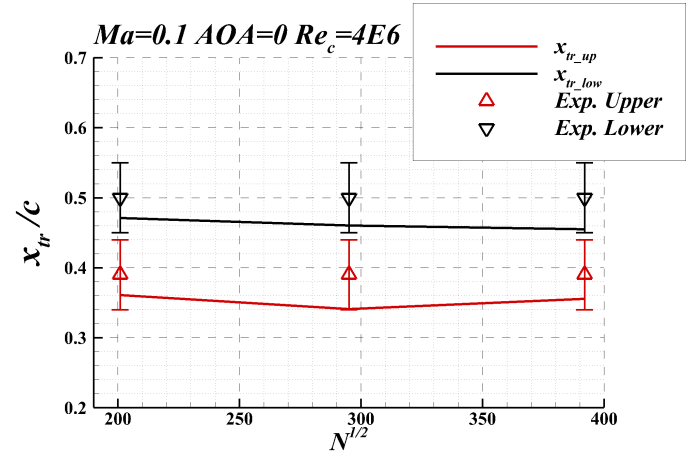

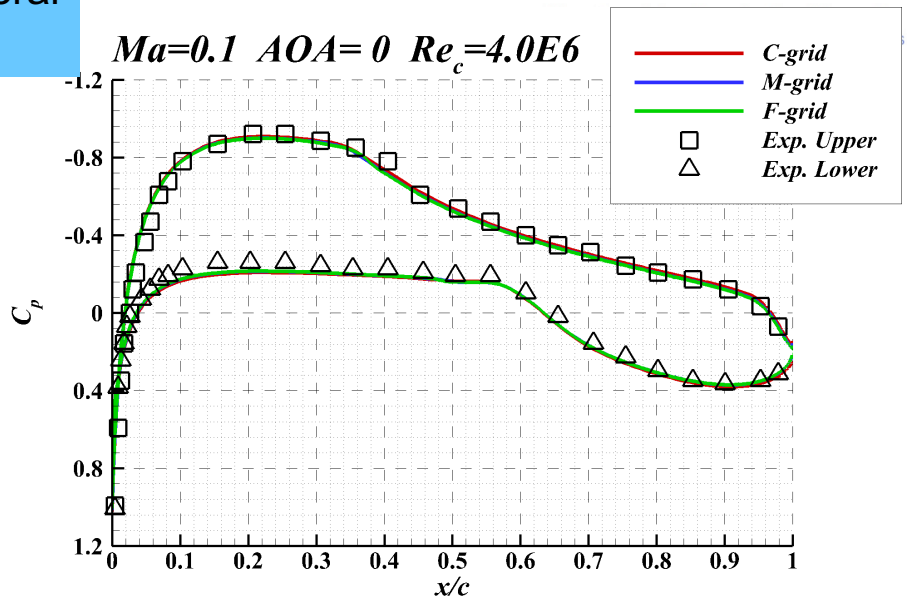

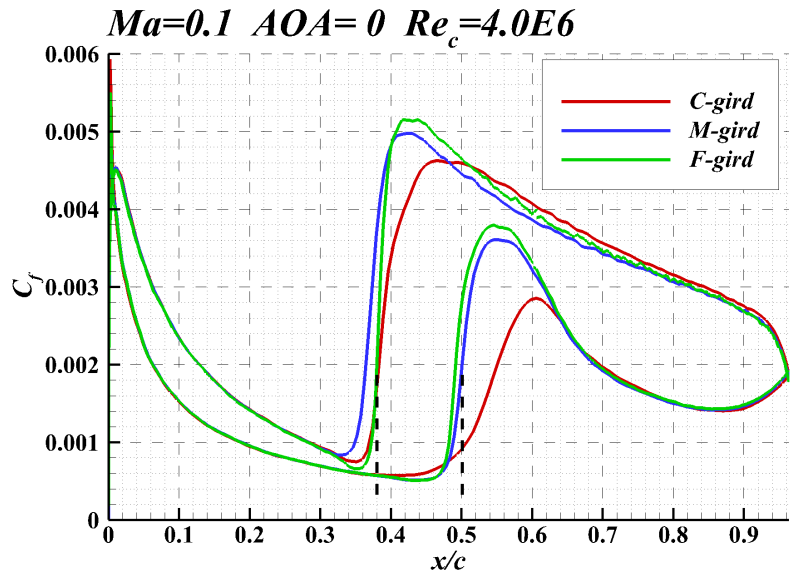

AoA=5 deg

- The maximum difference of transition onset on the lower surface is less than 2%C.

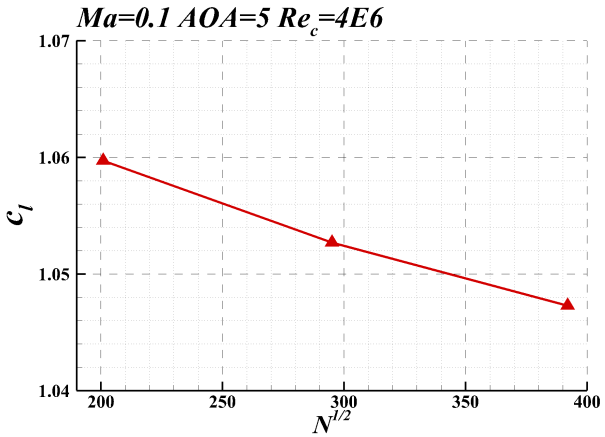

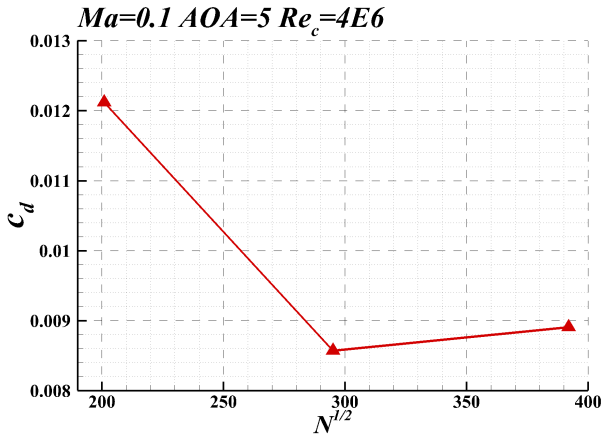

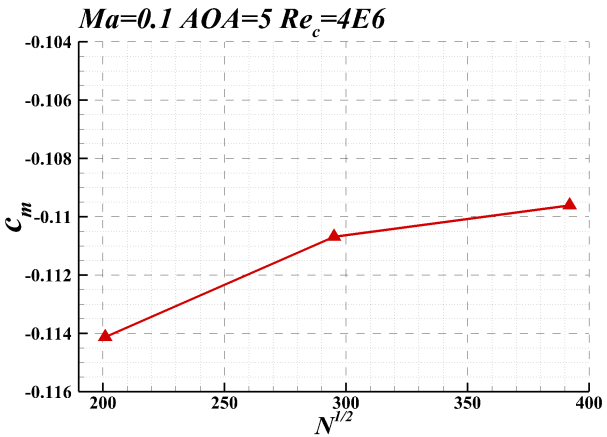

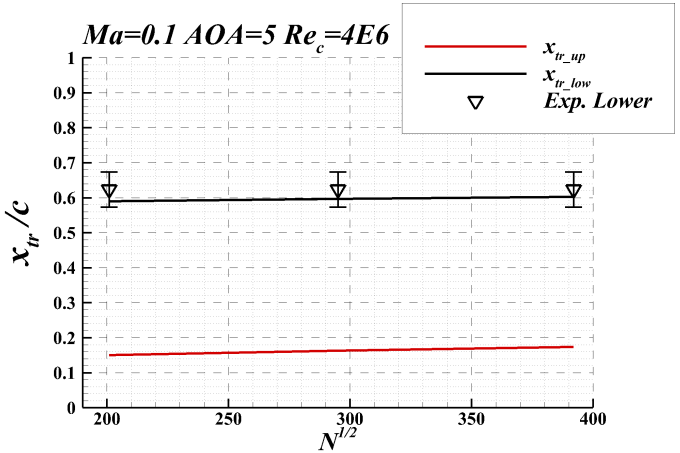

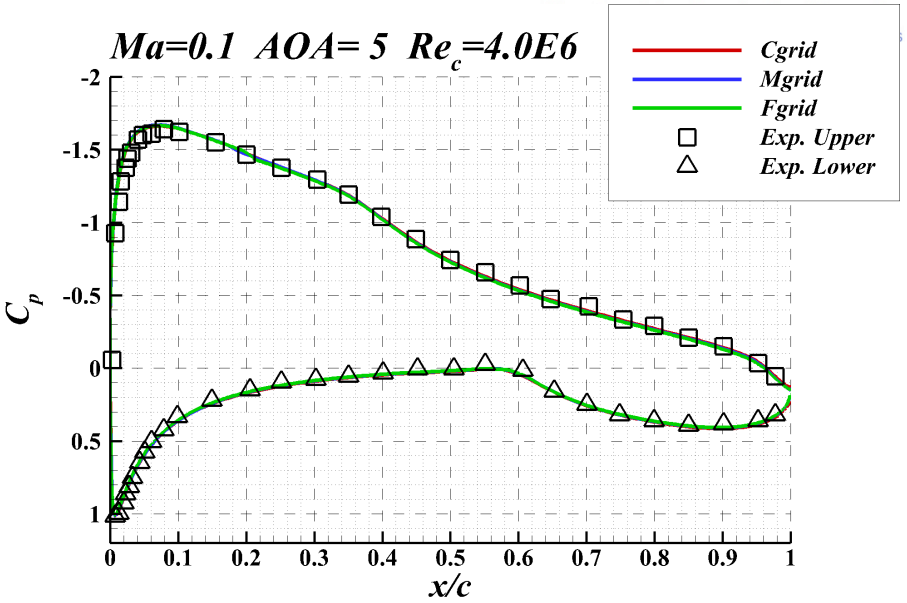

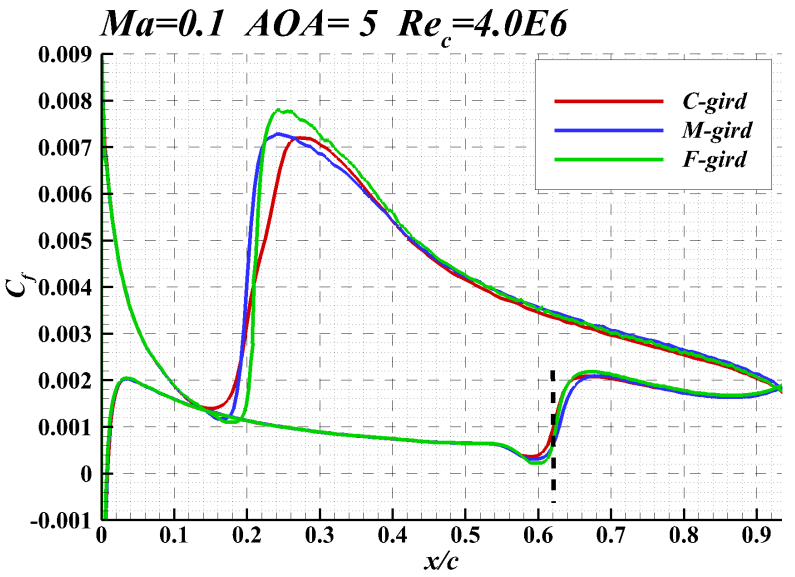

Comparisons of aerodynamics

- AOA=-4, -2, 0, 2, 4, 6, 8
  - C_l, C_d, C_m
- The drag by transition model matches the measurements better than FT model.

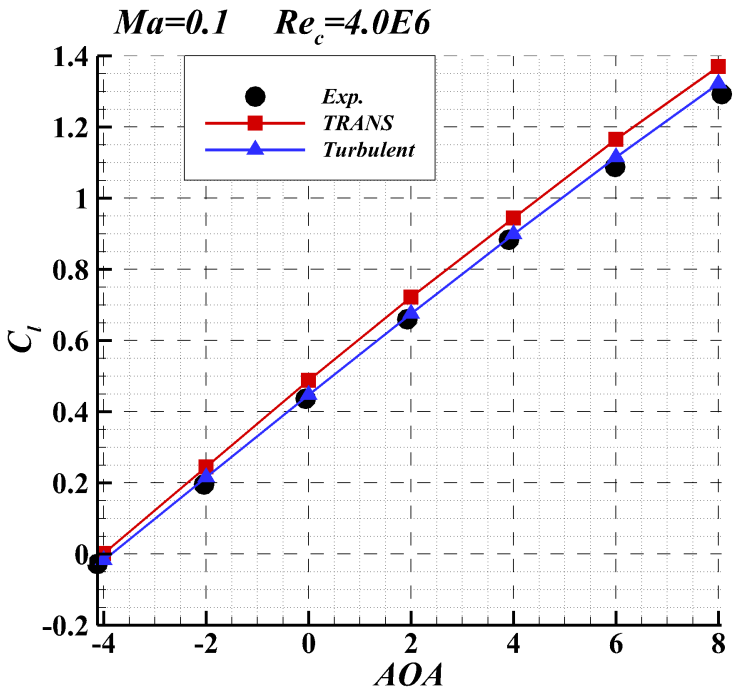

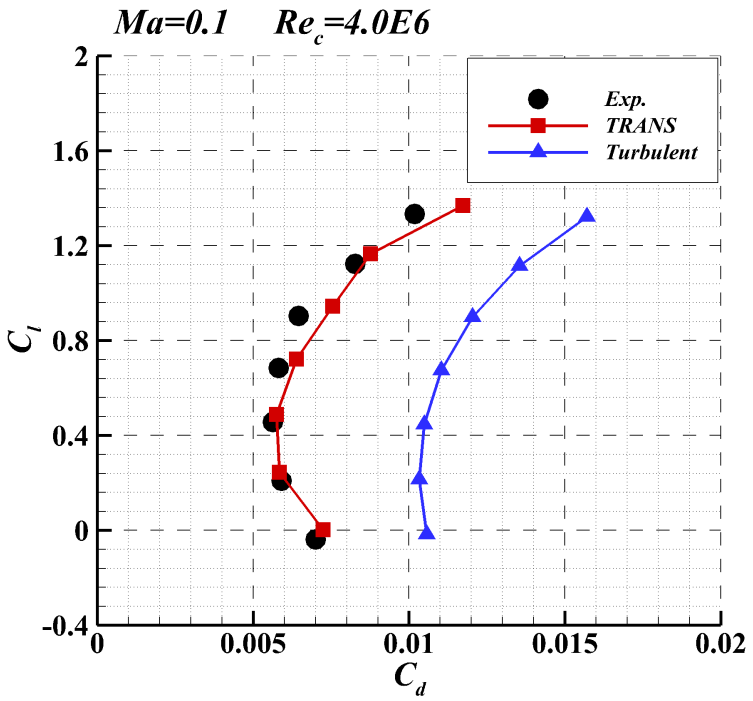

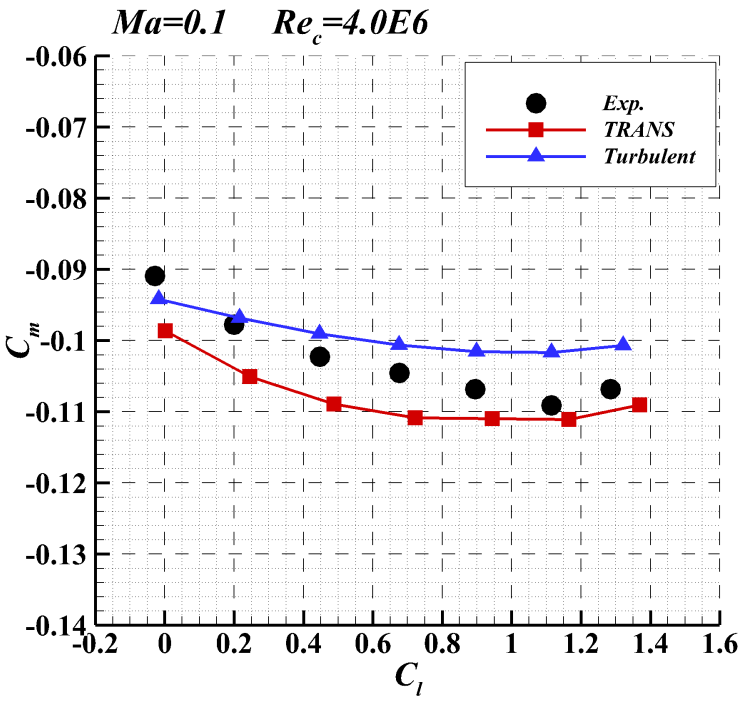

Comparisons of transition locations

- AoA=-4, -2, 0, 2, 4, 6, 8 deg
- With increase of AoA, the transition onset on the upper surface moves upstream, while it moves downstream on the lower surface.
- The maximum difference of transition onset is less than 3%C

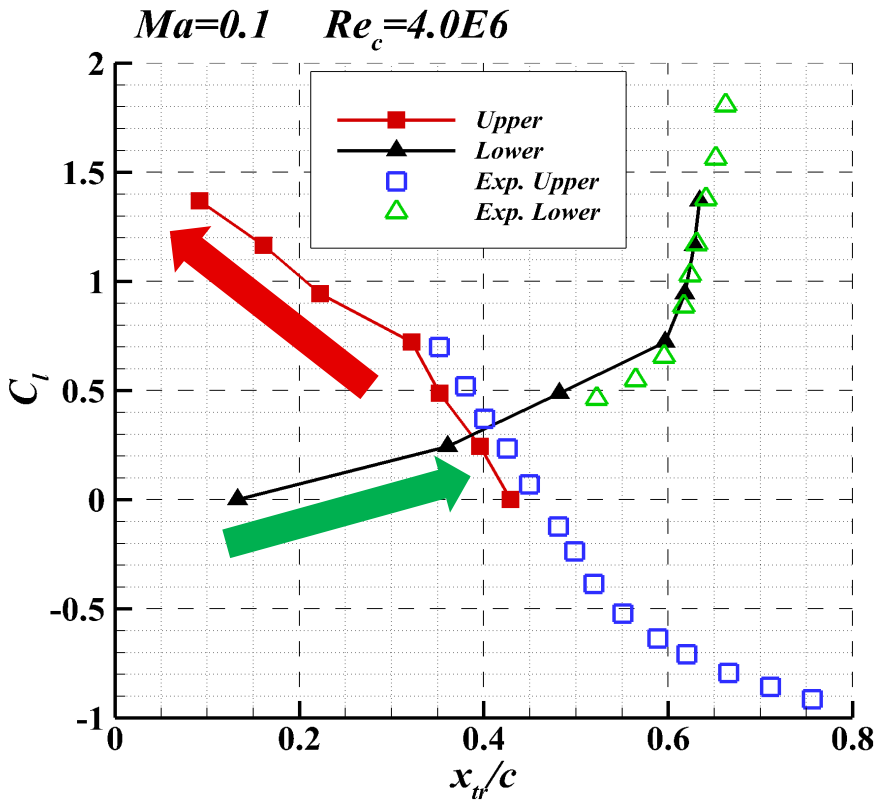

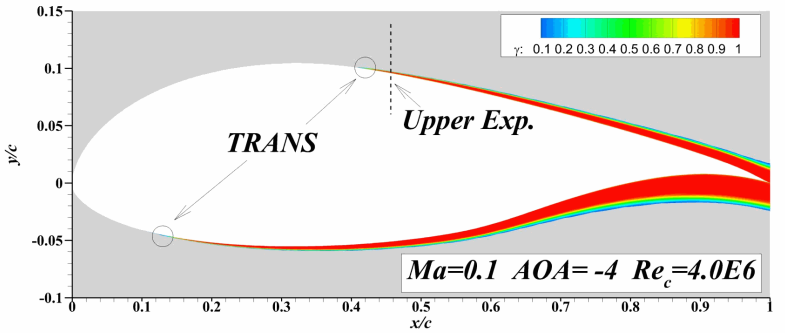

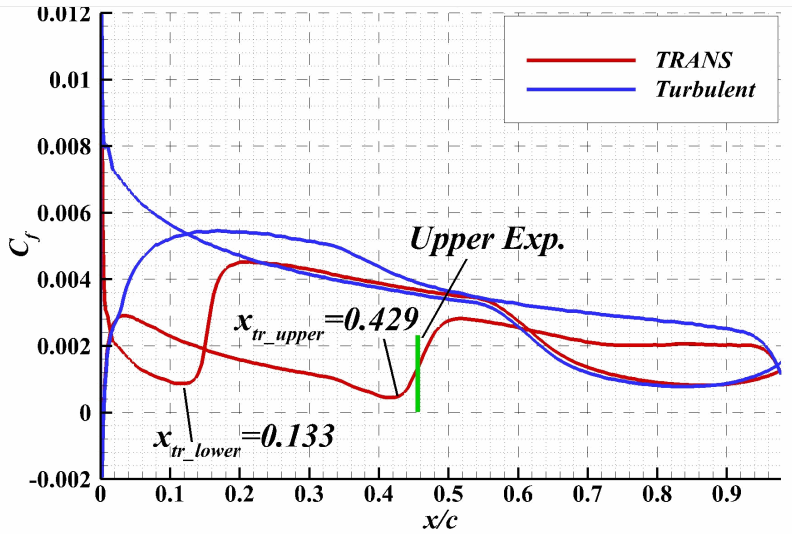

and prelimina

CASE3. 6:1 prolate spheroid

- Computational conditions
  - Ma=0.13, FSTI=0.15%, Re_L=6.5E6, T_∞=300K
    - AOA=5,10,15

The flow is the typical natural transition and dominated by both 1st and crossflow modes

- Grid & Boundary Conditions
  - Gird :N= 7,233,408
    - N_streamwise=347
    - N_normalwise=118
    - N_circumferential=193
  - BC: Wall & Farfield
    - Farfield > 100L

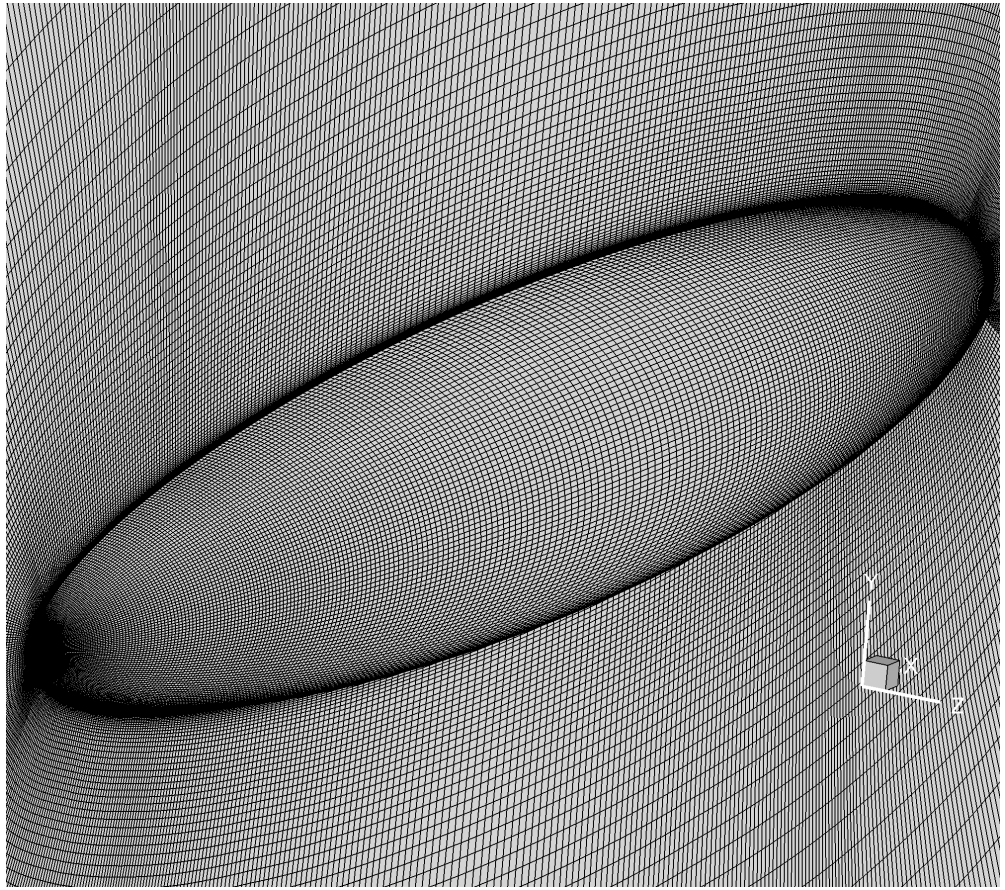

AoA=5 deg

Grabe C , Shengyang N , Krumbein A . Transition Transport Modeling for the Prediction of Crossflow Transition[C]// AIAA Paper, 2016-3572

- The transition occurs near 0.5L with small adverse pressure gradient and the crossflow is relatively weak.
- At PHI ≈ 90deg, $(\triangle x_{tr})_{max} \approx 0.1L$

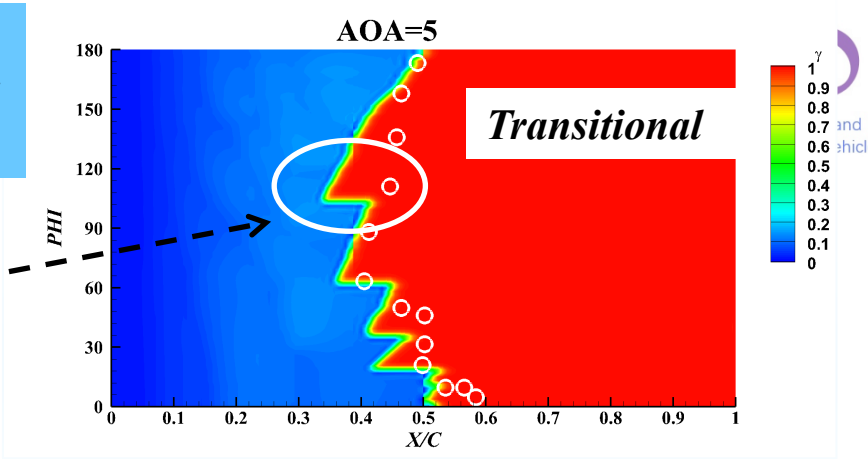

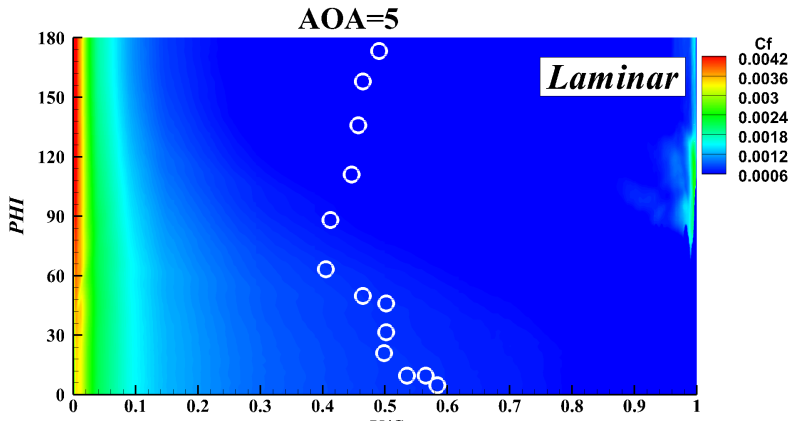

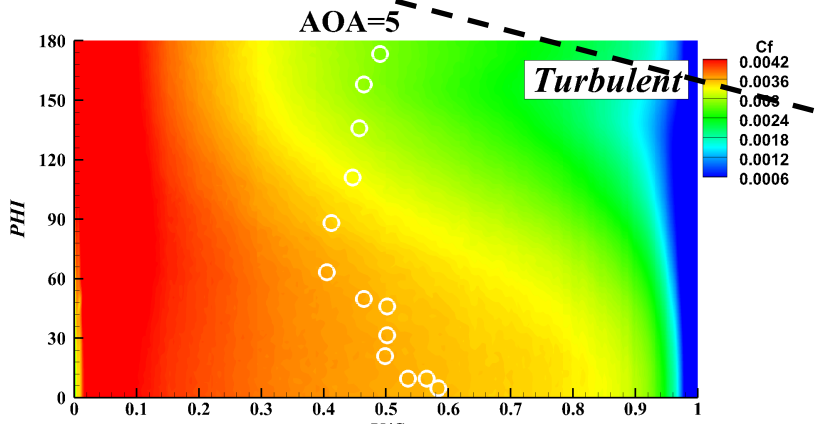

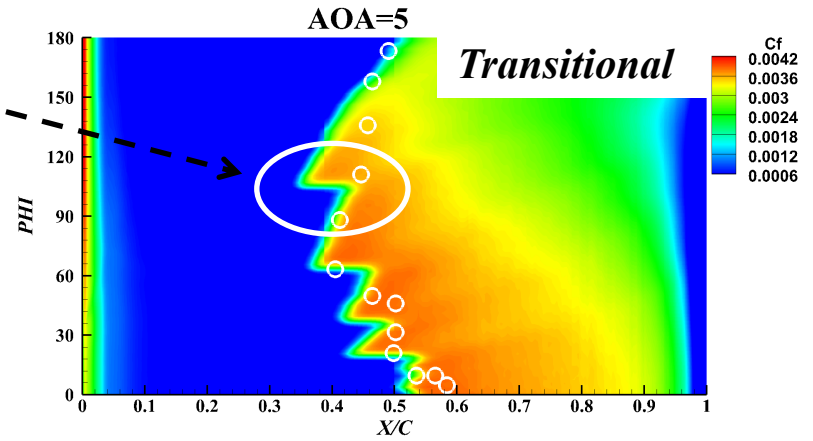

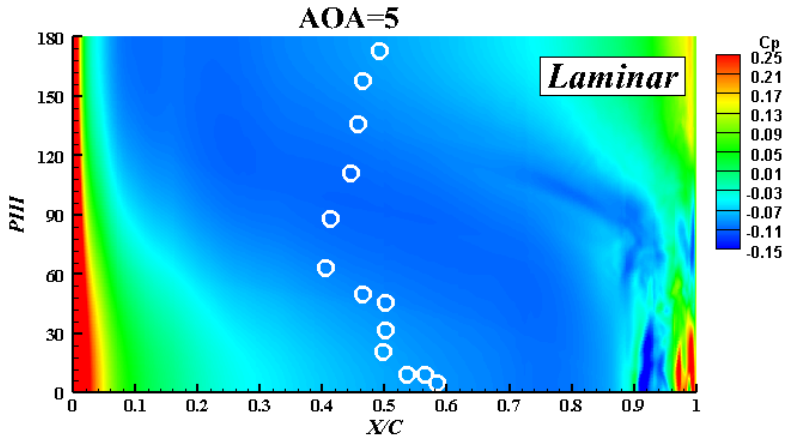

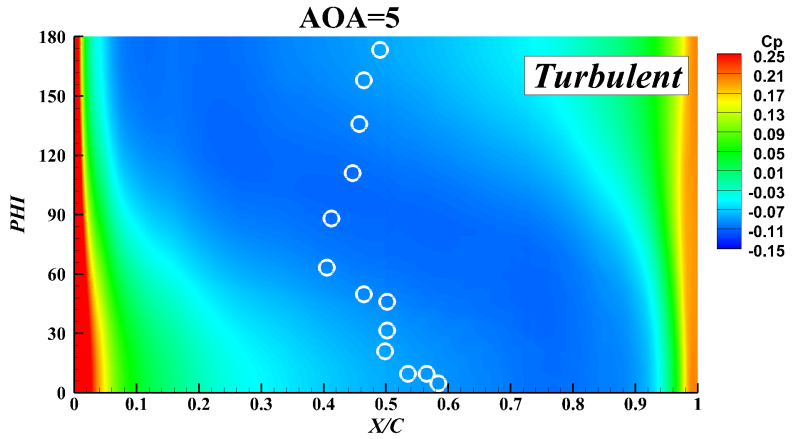

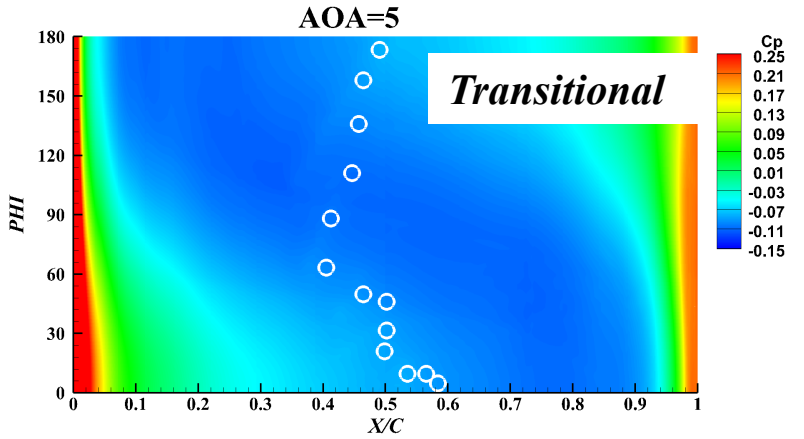

AoA=10 deg

- The pressure gradient increases and the transition onset moves upstream on the leeward side. The crossflow becomes stronger.
- At PHI of 20deg, $(\triangle x_{tr})_{max} \approx 0.15L$

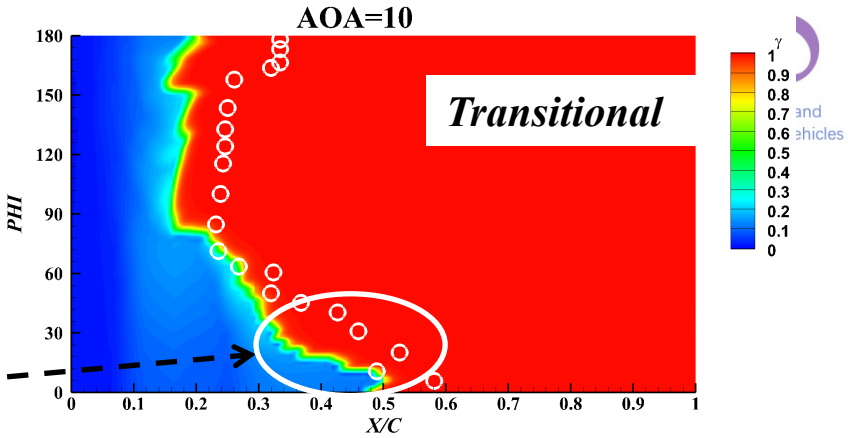

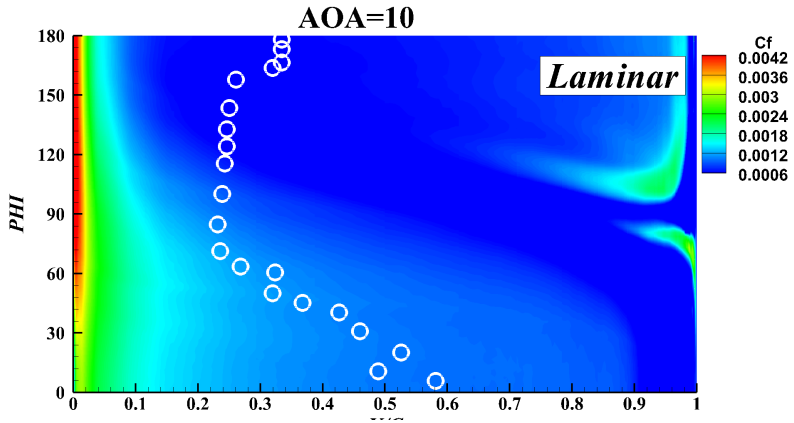

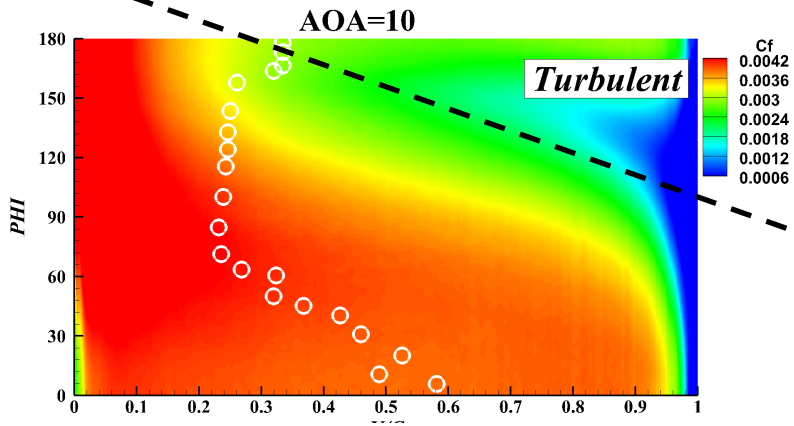

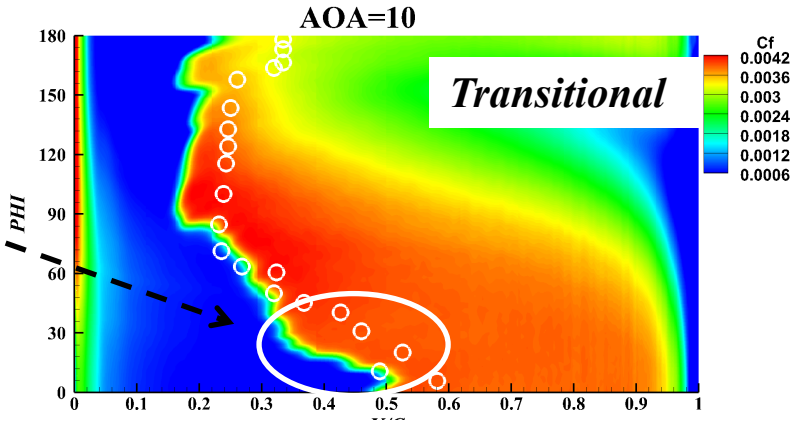

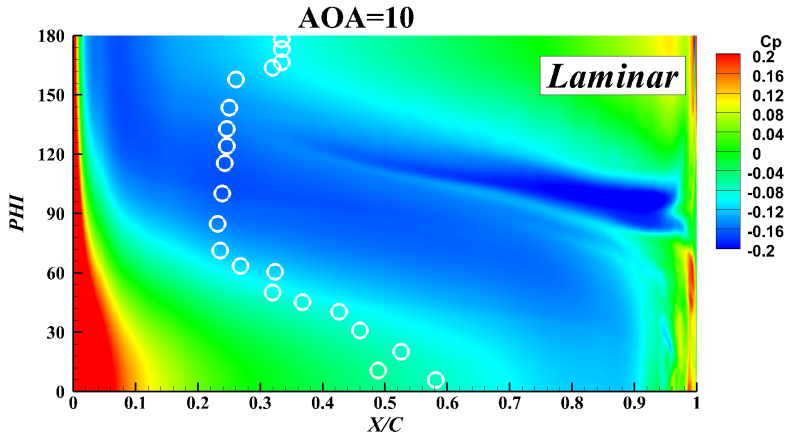

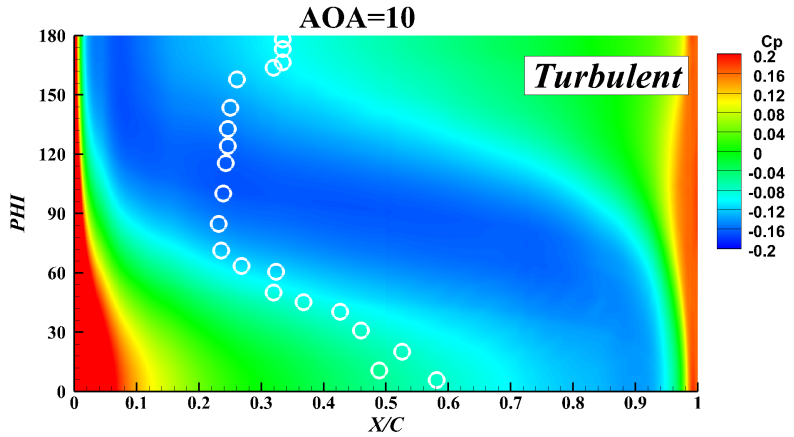

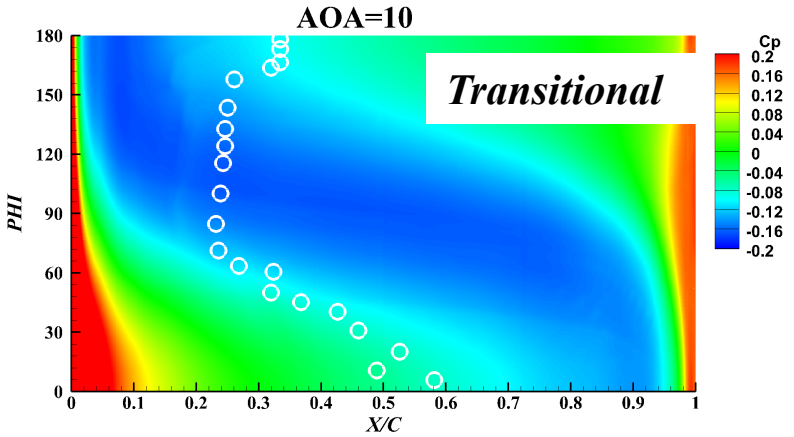

AoA=15 deg

- The transition onset on the leeward side is much more upstream than that on the windward side, with the largest AoA here.
- At Phi of 15 deg, $(\triangle x_{tr})_{max} \approx 0.15L$

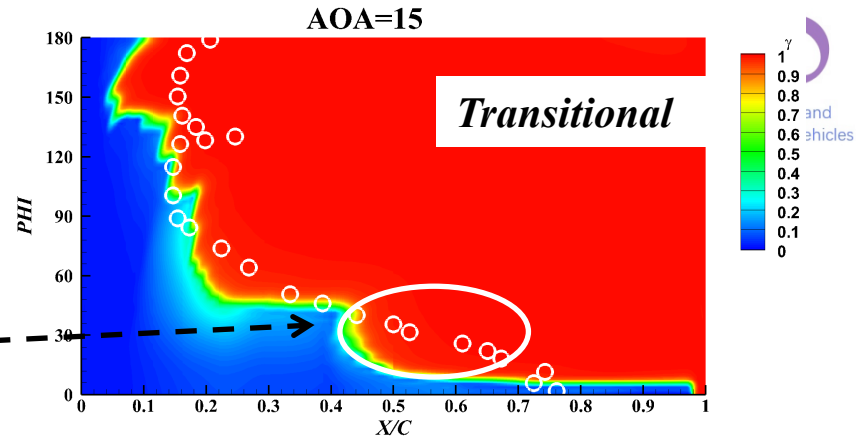

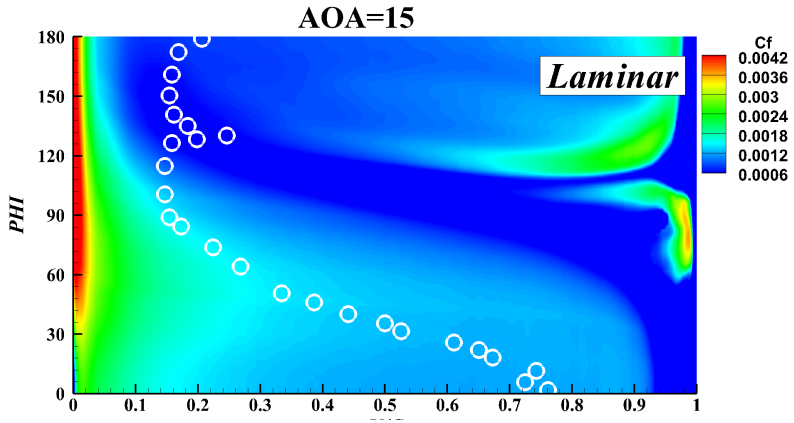

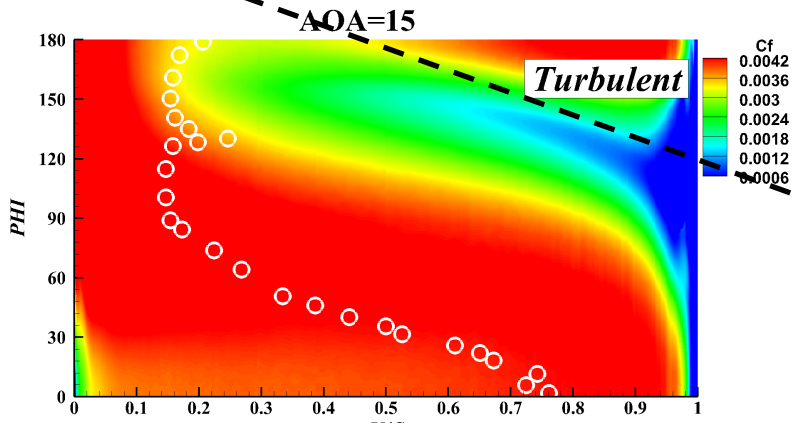

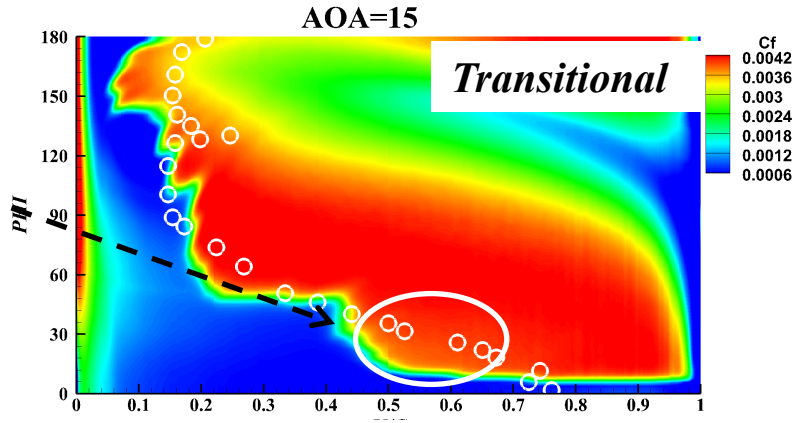

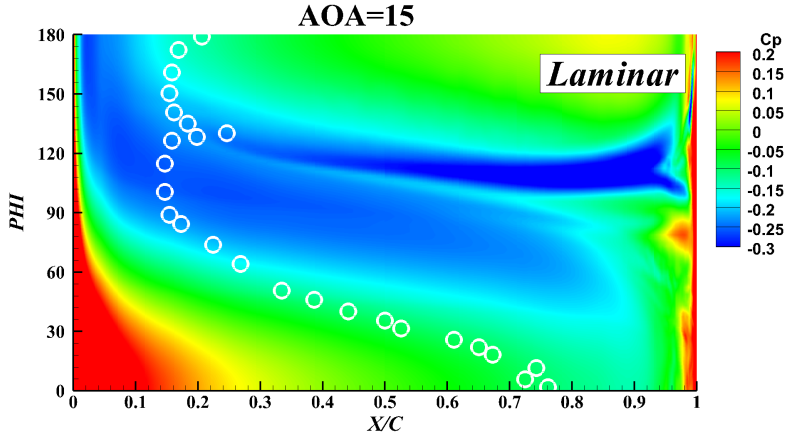

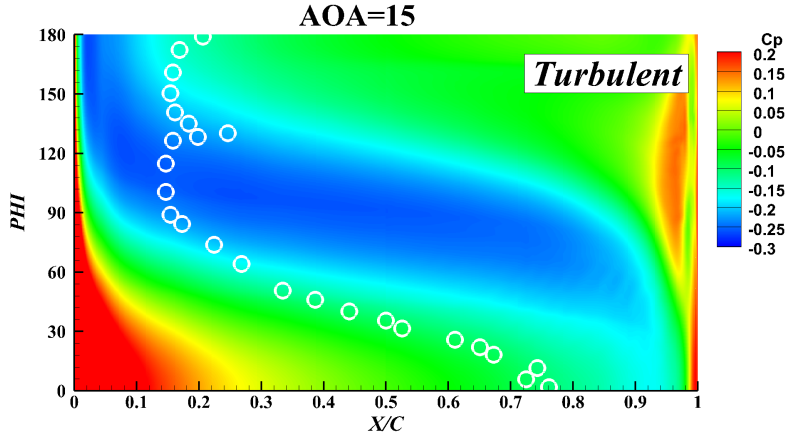

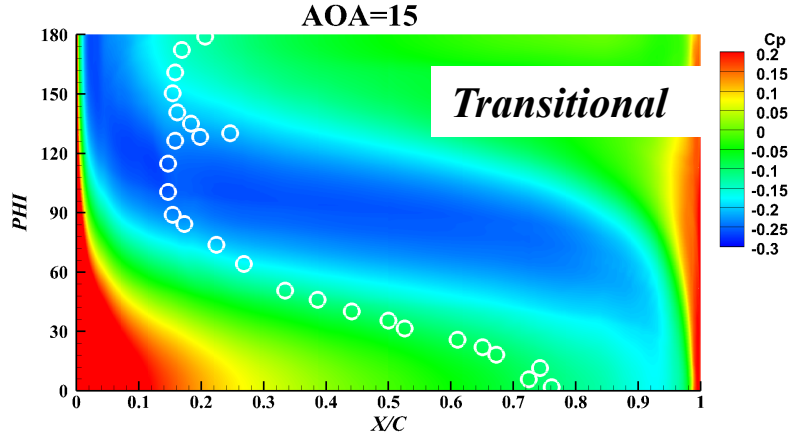

Distributions of time scale

- The location is at Phi=90deg, where the most upstream transition for 5, 10 & 15 deg.
  - AOA↑, Crossflow ↑
- The contribution to the transition of crossflow is much larger than 1st mode with increase of AoA.

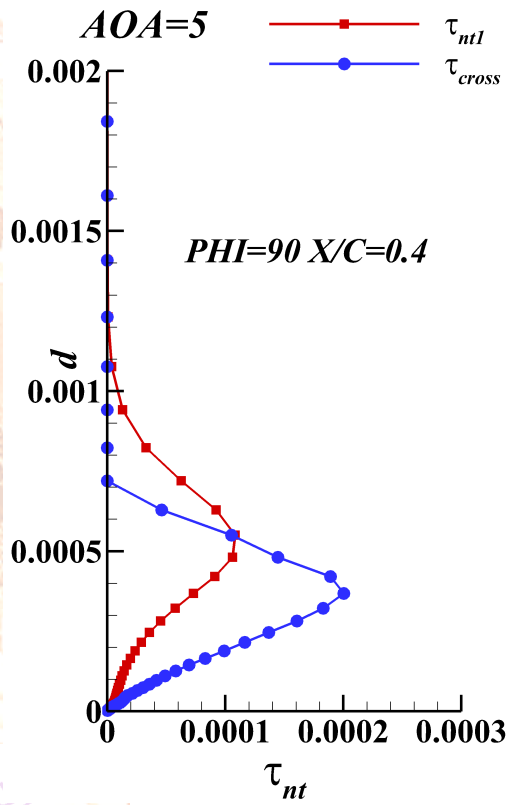

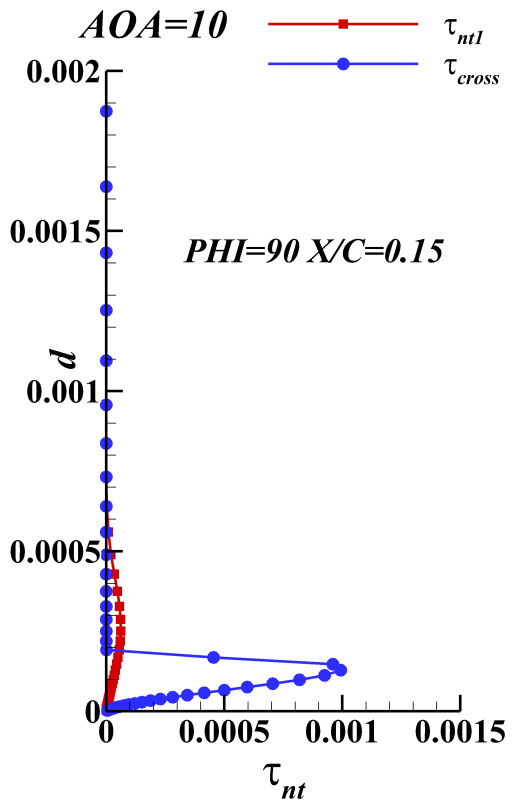

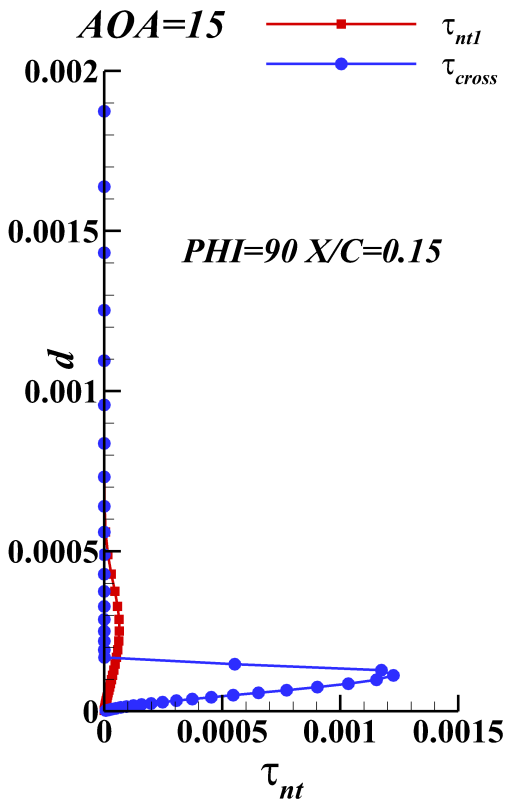

CASE4. preliminary results for CRM-NLF

- The flow is mainly dominated by 1st mode and the crossflow is relatively weak.
- Ma=0.86, Re_{MAC}=1.5E7, FSTI=0.24%
  - AoA=1.44848, 1.98031, 2.46141, 2.93787 deg
- Only about 5 million cells are used for half-model.
- The model agrees well with the Exp. of forces and pressure

Lynde M N, Campbell R L, Rivers M B, et al. Preliminary Results from an Experimental Assessment of a Natural Laminar Flow Design Method[C], AIAA Paper, 2019-2298, 2019.
Rivers M B, Lynde M N, Campbell R L, et al. Experimental investigation of the nasa common research model with a natural laminar flow wing in the nasa langley national transonic facility[C], AIAA Paper 2019-2189, 2019.

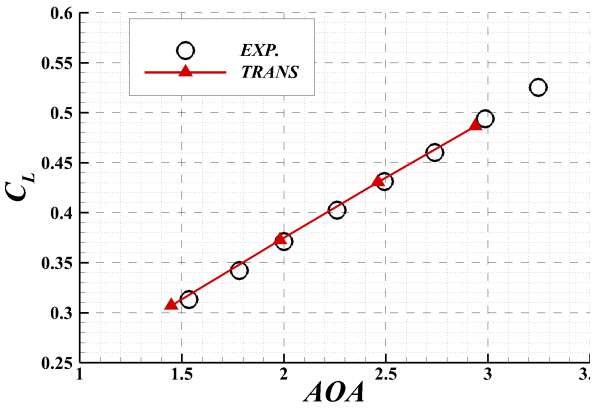

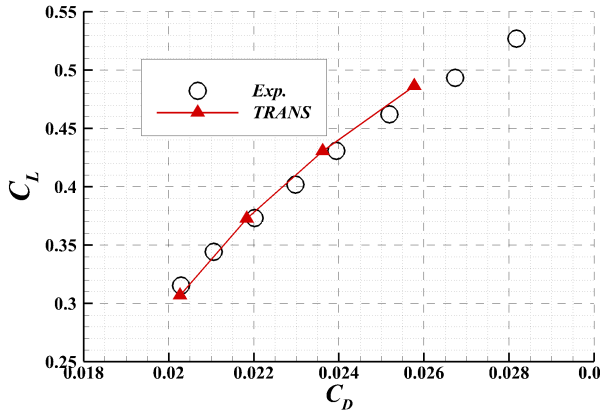

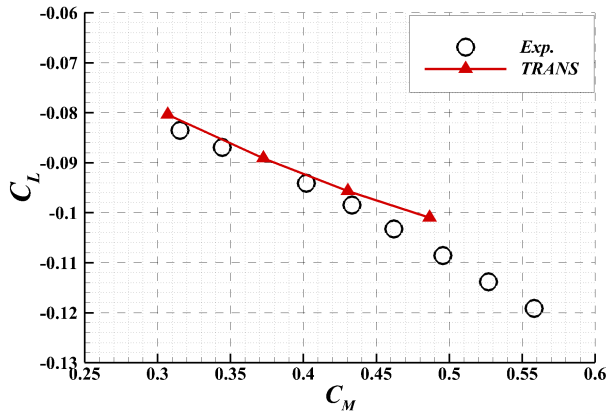

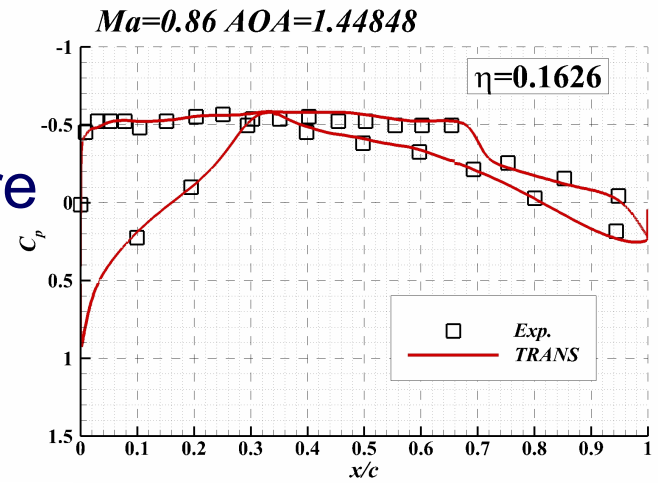

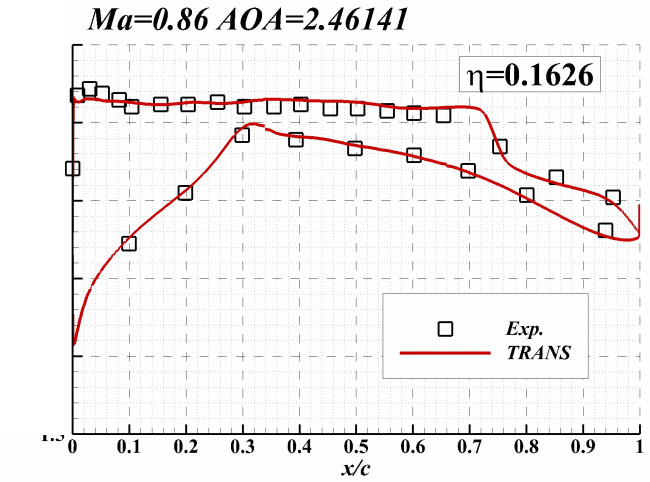

Transition at AoA=1.448 deg

- The numerical transition is much outer than the measurements in the spanwise direction, mainly caused by the over-predicted crossflow.
- Grid numbers should be increased and the mesh should be improved.
- Also the crossflow should be well predicted.

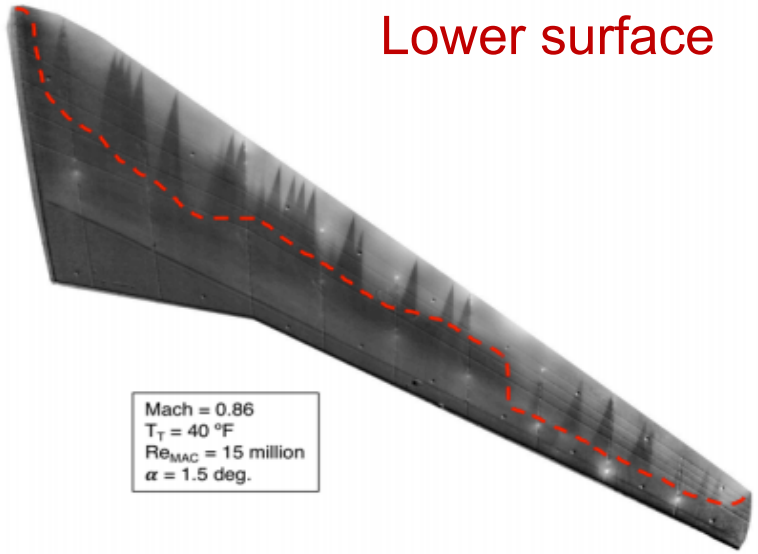

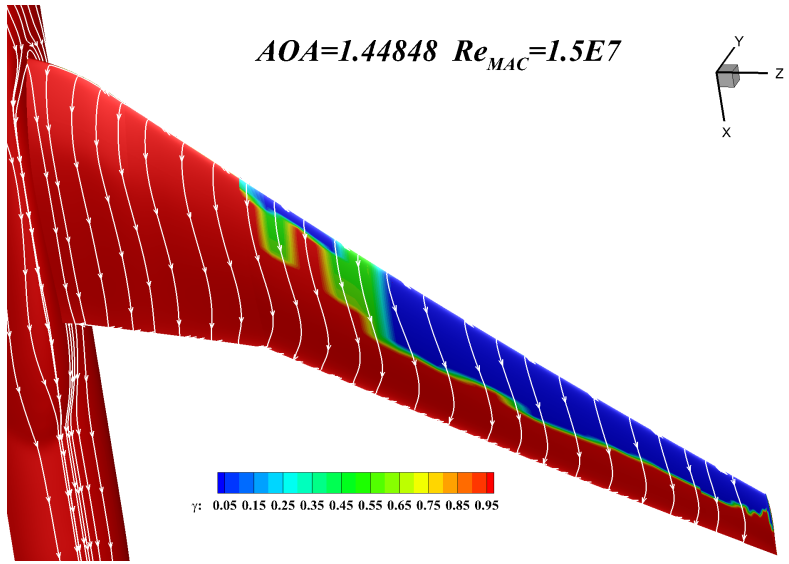

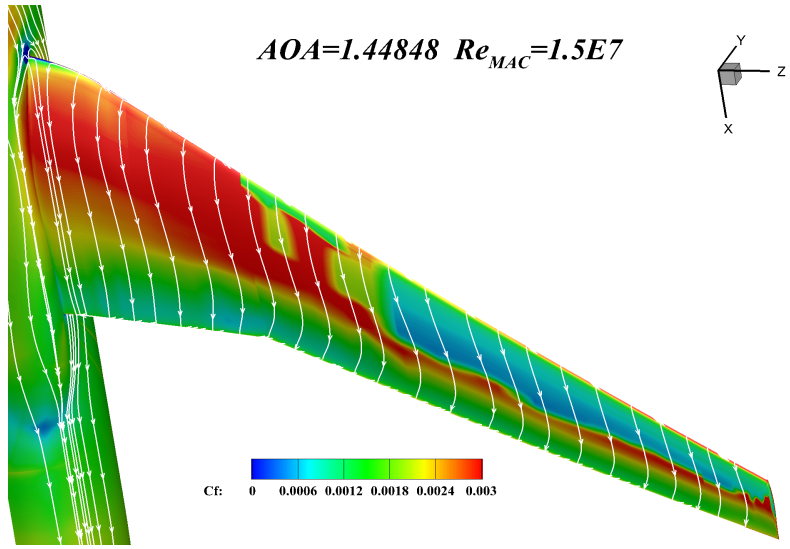

Four AoAs: 1.448, 1.98, 2.461 & 2.938

- The transition onset moves to the wing-tip with increase of AoA, mainly caused by the stronger crossflow.
- In the transitional region near the wing tip, the streamwise transition onsets vary little.

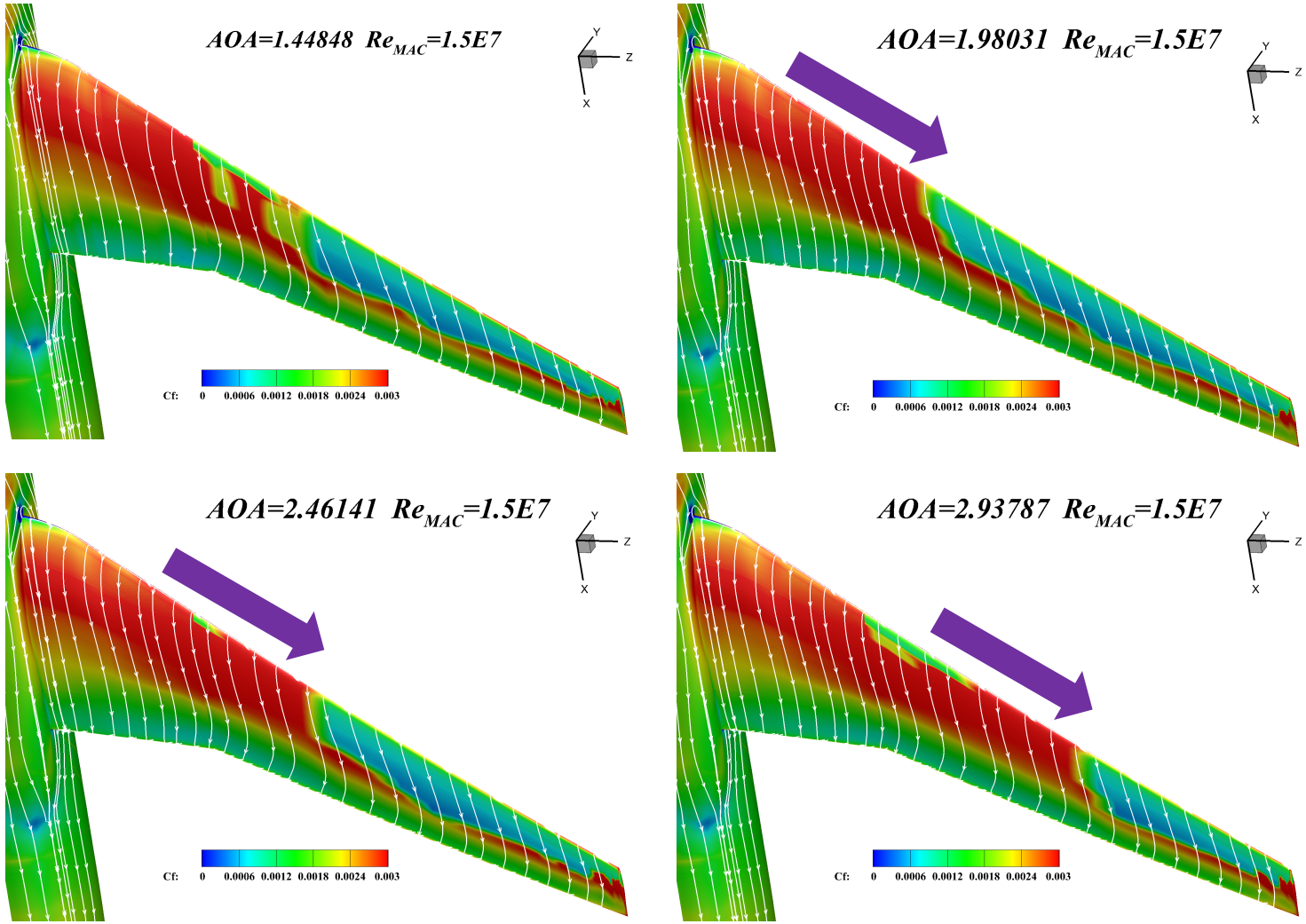

5. Conclusions

- A fully turbulent case and 4 transitional cases were simulated by the SST and 3-equ. k-ω-γ transition models, based on our in-house CFD software, TRANS;
- For the FT case, TRANS performs similar with CFL3D, except the eddy viscosity;
- For the transitional cases, the transition model can well predict the transition onsets with acceptable differences between the sim. and measurements;
- For the transonic case past the CRM-NLF, further work shall be implemented in the future.

- Acknowledges
  - This work was supported by the National Key Research and Development Program of China (Grant No. 2016YFA0401200 and 2019YFA0405300). This was also supported by the National Key Project (Grant No. GJXM92579), and the National Natural Science Foundation of China (Grant Nos. 91952302, 11772174 and 91852113).

清華大學
Tsinghua University

THANKS FOR YOUR ATTENTIONS!

ZHIXIANG XIAO
XIAOTIGERZHX@TSINGHUA.EDU.CN

Wechat Public Number

LAD

*L*aboratory of *A*erodynamics *S*imulation and preliminary *D*esign for innovative aero-vehicles